UNITED STATES DEPARTMENT OF THE INTERIOR

GEOLOGICAL SURVEY

Self-Potential Measurements and Interpretation at Rivière Langevin and Cirque de Salazie, Ile de la Réunion

by

David V. Fitterman

Open-File Report 82-580

1982

Contents

	Page
1. Introduction	1
1.1 Equipment	1
1.2 Procedure	4
1.3 Measurement noise	4
1.4 Data treatment	5
2. Rivière Langevin and Plaine des Sables	6
2.1 General characteristics of the SP anomaly	7
2.1.1 Division of data by anomaly (A) type	11
2.1.1.1 Anomalies associated with water flow (A1)	11
2.1.1.2 Anomalies not associated with water flow (A2)	12
2.1.2 Division of data by correlation with topography (T)	12
2.2 Interpretation of the anomalies	16
2.2.1 Interpretation of region A1 anomalies	18
2.2.2 Interpretation of region A2 anomalies	26
2.3 Summary of results	36
3. Cirque de Salazie	37
3.1 Treatment of the data	37
3.2 General characteristics of the SP data	40
3.3 Comparison of SP anomaly with DDR data	40
3.4 Summary of results	46
4. Conclusions	47
Acknowledgment	49
References	50

1. Introduction

During a three week period in April and May 1981, self-potential (SP) measurements were made on the Ile de la Réunion in two regions being studied for their geothermal energy potential by the Département Géothermie of the Bureau du Recherches Géologiques et Minières (B.R.G.M.). The Ile de la Réunion is an active volcanic island located 800 km east of Madagascar in the Indian Ocean (Figure 1). The first area surveyed was in the Rivière Langevin to the west of Piton de la Fournaise (Figure 2). The profile ran alongside the river and was continued northward onto the Plaine des Sables. A short profile perpendicular to the first line was also made on the plain. The second area of investigation was centered around the village of Salazie in the Cirque de Salazie. The survey began north-east of Salazie and proceeded toward the village of Salazie and then branched in two directions. The first extension went in the direction of Grand Ilet, while the second extension passed through the village of Hell-Bourg toward Ilet à Vidot. In all, 859 measurements covering about 43 km were made.

1.1 Equipment

The equipment used for the measurements was standard, and included the following items: (1) a high input impedance (10MΩ) voltmeter (Danameter Model 2000A); (2) non-polarizable $Pb-PbCl_2$ electrodes which were provided by the Centre de Recherches Géophysiques, Garcy (Petiau and Dupis, 1980); and (3) 5 km of light-weight cadmium-bronze wire. When conditions did not permit the use of a long cable, a 60 m length of heavier gauge cable was used.

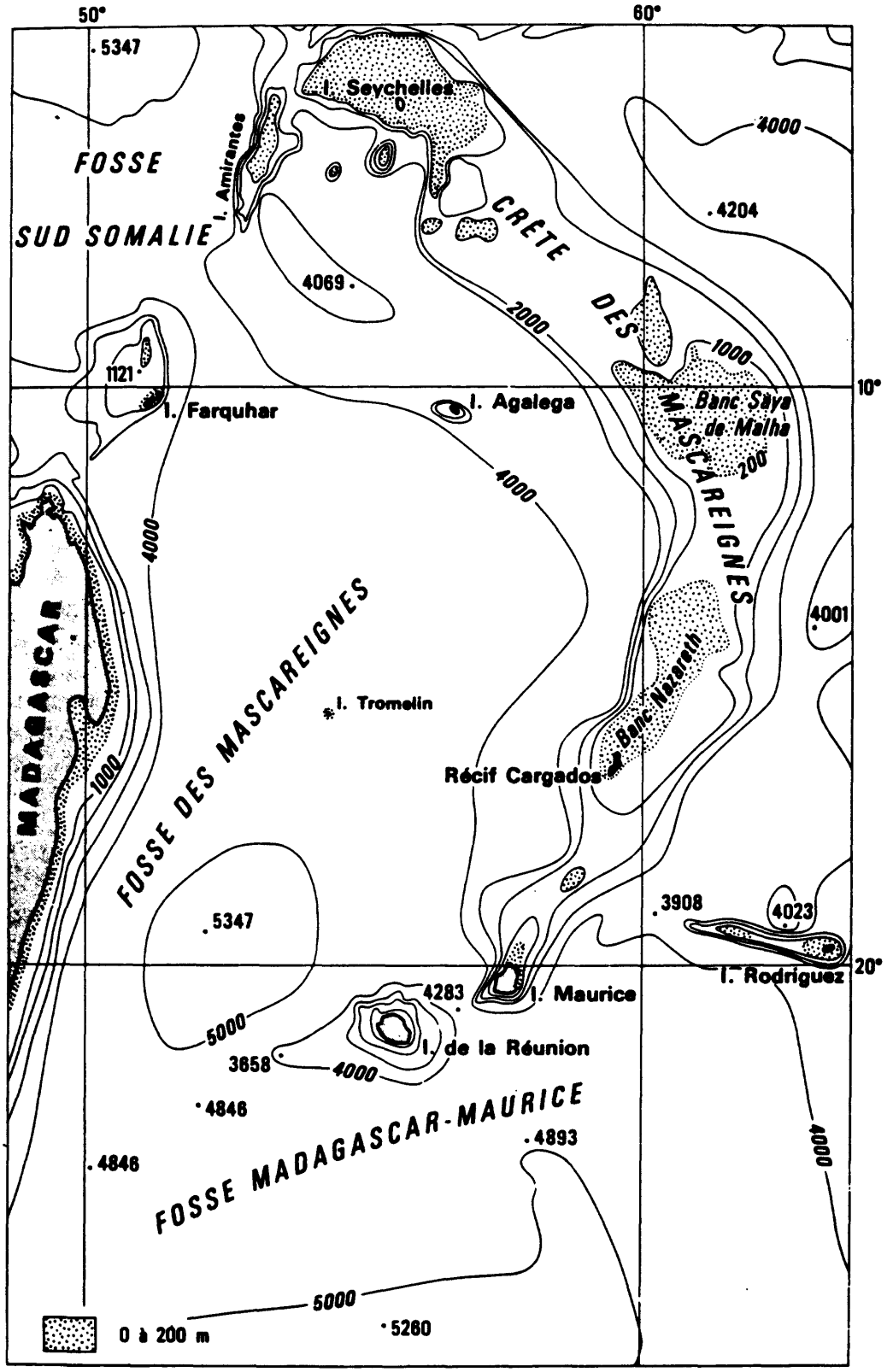

CARTE BATHYMÉTRIQUE DE SITUATION

1. Location map of Ile de la Réunion. Contours are water depth in meters (after, Billard, 1974).

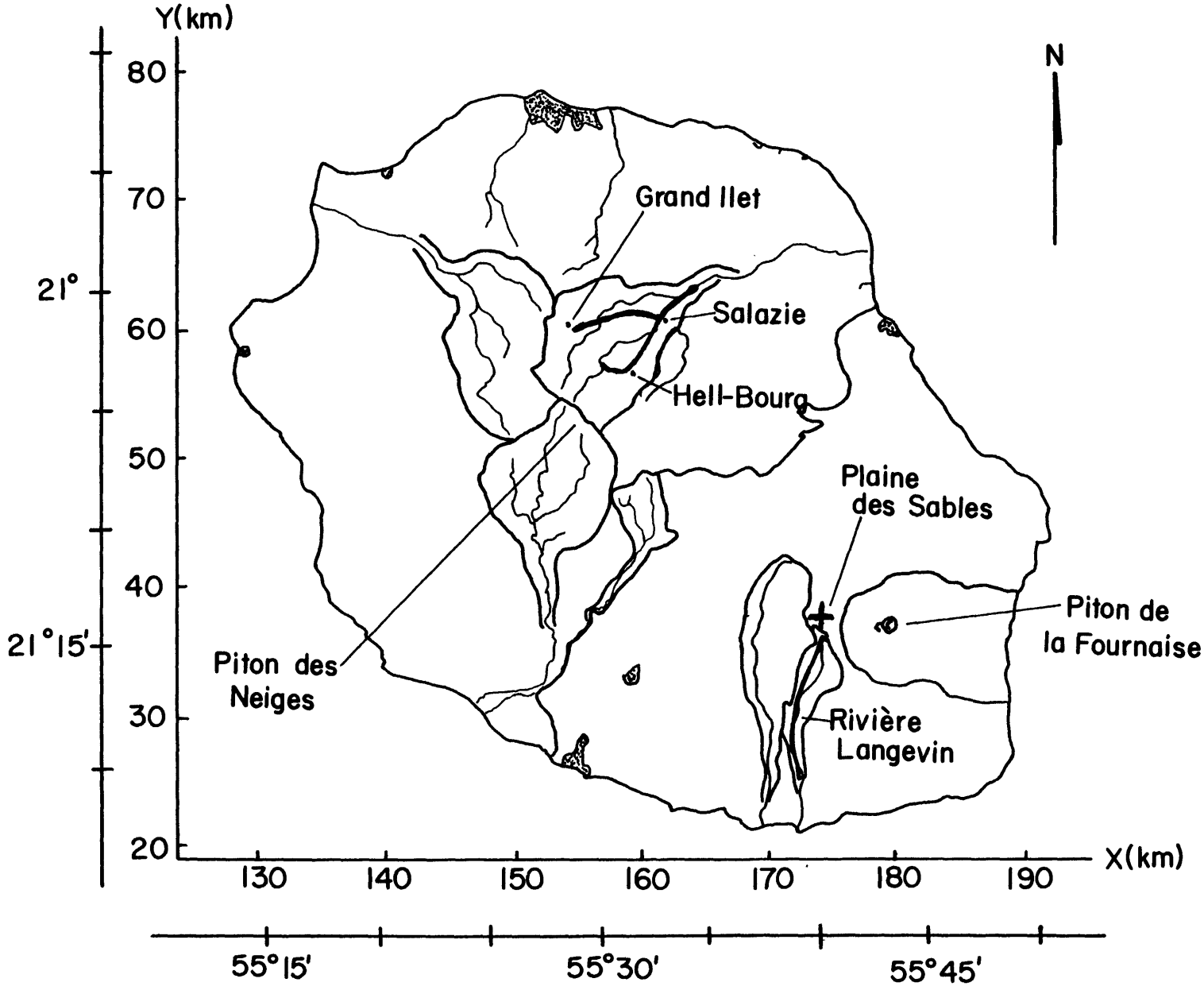

2. Location map of SP traverses on the Ile de la Réunion. Heavy lines indicate the survey lines. The horizontal and vertical scales are in kilometers.

1.2 Procedure

When possible the measurements were made using a fixed reference electrode and a portable electrode connected to each other by a long wire ("la méthode grande ligne"). The usual distance between measurements was 50 meters. At the measurement point a small hole was made, and the soil in the bottom of the hole was lightly tamped to provide a flat surface on which to place the electrode. There was usually sufficient moisture in the soil to make a low-impedance contact. However, if the contact impedance was high, a small amount of a mixture of soil, water, and salt, which had the consistency of "crème fraiche" was placed in the bottom of the hole. The contact impedance was quickly measured after the voltage measurement to be sure the contact impedance was low. This test was also made when we suspected that the wire had been cut. A cut cable was obvious because the normally stable voltages (drift of much less than 1 mV/minute) became very erratic. Frequent cutting of the cable by the children often required the use of the leap-frog measurement technique ("saute-mouton") with all of its attendant noise problems. This technique was also used in regions of difficult terrain which we did not want to traverse more than once.

1.3 Measurement Noise

Three types of noise are considered possible in the data. The first noise is that due to changes in soil type or chemistry. This type of noise was evident when the measurement electrode was moved to other points within a meter of each other. This noise contributes a random error estimated to be about 10 mV at each measurement point. The second type of noise is due to cultural effects like buried pipes, concrete structures, or electrical power line poles. These noise sources tend to produce short-wavelength large-

amplitude spikes in the data which can be as great as 100 mV. Any large amplitude anomalies shorter than about 200 m are probably due to this effect. When possible, locations which displayed any of these noise sources were avoided; however, on several occasions this was not possible. The last type of noise, which can be present when the long wire method is used, is that due to telluric currents. The steady nature of all of the measurements, even when a line length of 3 km was used, makes me believe that the data are free of this type of noise.

1.4 Data Treatment

Several procedures have been used to reduce the effect of noise in the data. The effect of random measurement noise is minimized by using a running average filter on the data of the form

$$y(i) = \frac{1}{N} \sum_{j=o}^{N-1} x(i - j) = \langle x(i) \rangle_N \qquad (1)$$

where x(i) and y(i) are the raw and filtered data respectively. A filtering operation of this type lowpass filters the data. This filter also introduces a phase shift which is undesirable. By filtering the data first in the forward, and then in the reverse direction all phase shift is eliminated. Experimentation has shown that using a filter length of about eight eliminates much random noise while maintaining long wavelength features of the data which are considered important.

A second problem with the data is the existence of an inverse correlation with elevation. This is undoubtedly due to a streaming potential mechanism driven by the descent of water through the rocks. When the effect is small and constant, it can be removed by fitting a straight line to the data as a function of elevation. This correction function is then applied to the data. A correction of this type should be made before the data are lowpass filtered to avoid introducing kinks in the data.

The method of elevation correction described above does not work if there are distinct regions in the voltage-elevation plots with different slopes. In these cases one must apply a different linear correction to each region or use a filtering method to remove this regional effect. If we assume that the regional effect varies much more slowly than the anomalies we are interested in, we can subtract from the original data the data which have been low-pass filtered. This is done using the running average process shown before as follows:

$$y(i) = \langle x(i) \rangle_N - \langle x(i) \rangle_M \qquad (2)$$

where M is bigger than N. For example, typical values are about eight for N, and M between 20 and 50. The second term of the above equation represents the regional effect, while the first term is the regular noise reduction filter. This approach of reducing the regional effect has not been exceedingly successful.

2. Rivière Langevin and Plaine des Sables

Self-potential measurements were made along the Rivière Langevin starting at a point about 4 km north of the coast (Pointe de Langevin) and stopping at the southern edge of the Plaine des Sables (Figure 2). A second line continued 2 km farther north on the Plaine des Sables. While the potential was not measured between the northern point of the first line, and the southern point of the second line, it has been assumed to be zero. This was accomplished by adding an appropriate bias value to all of the data from the Plaine des Sables. This north-south profile will be referred to as Rivière Langevin even though the data between distances 14 km and 16.05 km are in fact on the Plaine des Sables.

A third line, perpendicular to the Rivière Langevin profile, was made on the Plaine des Sables from the base of the western ramparts to the summit of Piton Chisny. This profile is called Plaine des Sables.

Dipole-dipole resistivity (DDR) measurements were made by a B.R.G.M. crew along the same route as the Rivière Langevin SP profile. The location of the SP and DDR profiles is shown in Figure 3.

2.1 General characteristic of the SP anomaly

The SP data and topographic profiles from the Rivière Langevin and Plaine des Sables profiles are shown in Figures 4 and 5. The Rivière Langevin data have been filtered using an averaging length of 8, while the Plaine des Sables data are unfiltered. The most striking feature of the data is the large amplitude of the anomaly. There is a voltage difference of about 1500 mV on the Rivière Langevin profile, and the voltage difference on the Plaine des Sables profile is almost as large (1300 mV). Most of the voltage change on the first profile is confined to the region between 10 km and 14 km. There is also a small anomaly near the 12 km point. The region from 0 km to 10 km has much smaller but significant voltage variations.

Examining the topographic profiles one obtains an idea of the cause of the large anomalies. The large decreases of potential are associated with the zones where the elevation increases. Water flow under the influence of gravity would produce an anomaly similar to the observations. The aquifer system is charged by rainwater on the Plaine des Sables - the region between 14 km and 16 km. Rain and fog are common in this region. The water percolates downward through the underlying basalt flows. Due to enhanced lateral permeability or an impermeable zone at a greater depth, the flow is forced to move horizontally to the south. The stream channels from the south

3. Location map of SP and DDR traverses near the Rivière Langevin and the Plaine des Sables. The horizontal and vertical scales are in kilometers and refer to the scales in Figure 2.

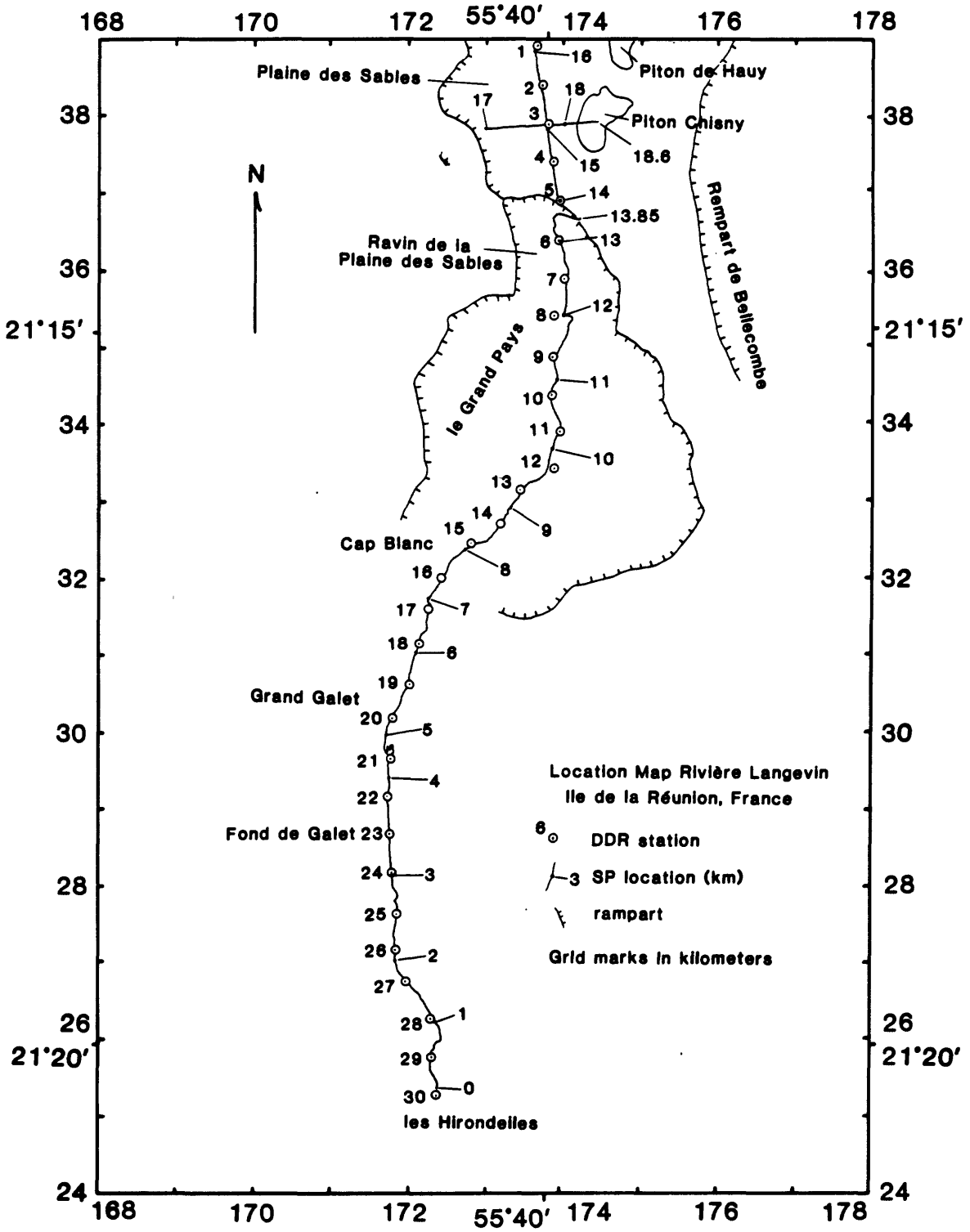

4. SP data and topographic profile from the Rivière Langevin. Data have been filtered with a filter length of 8.

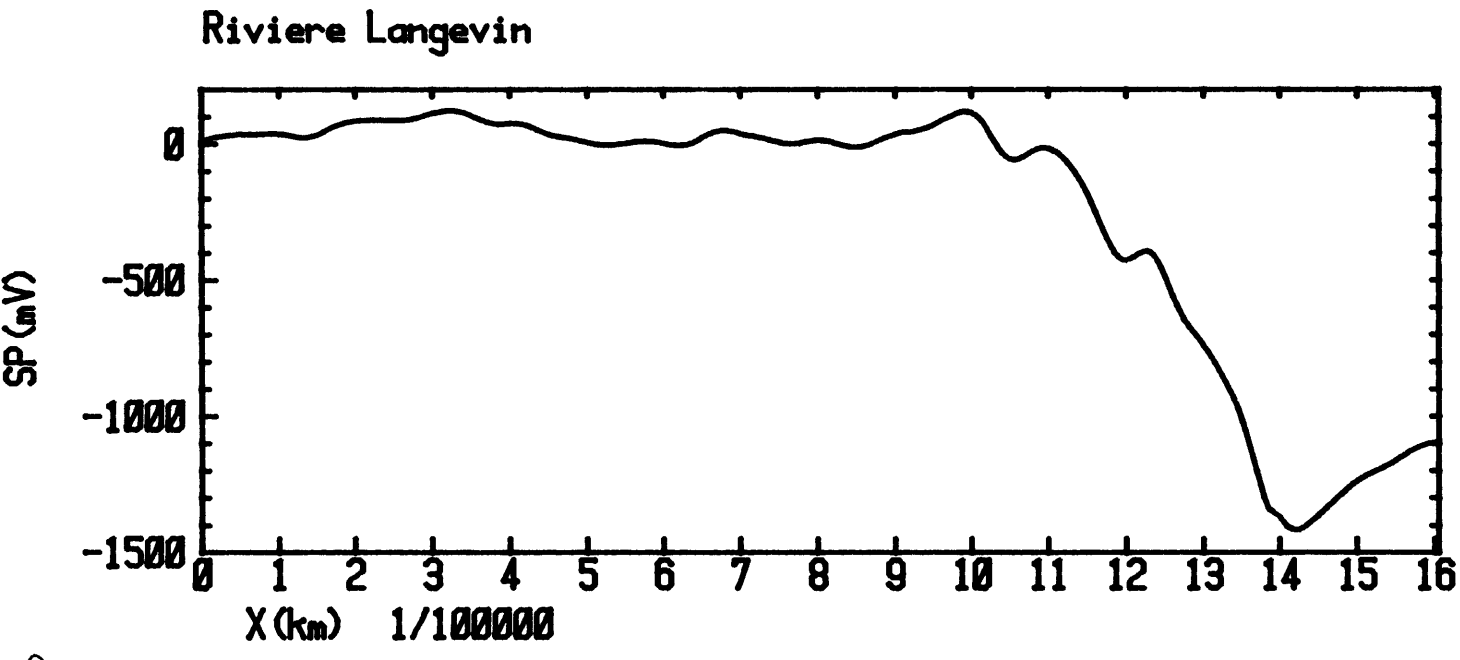

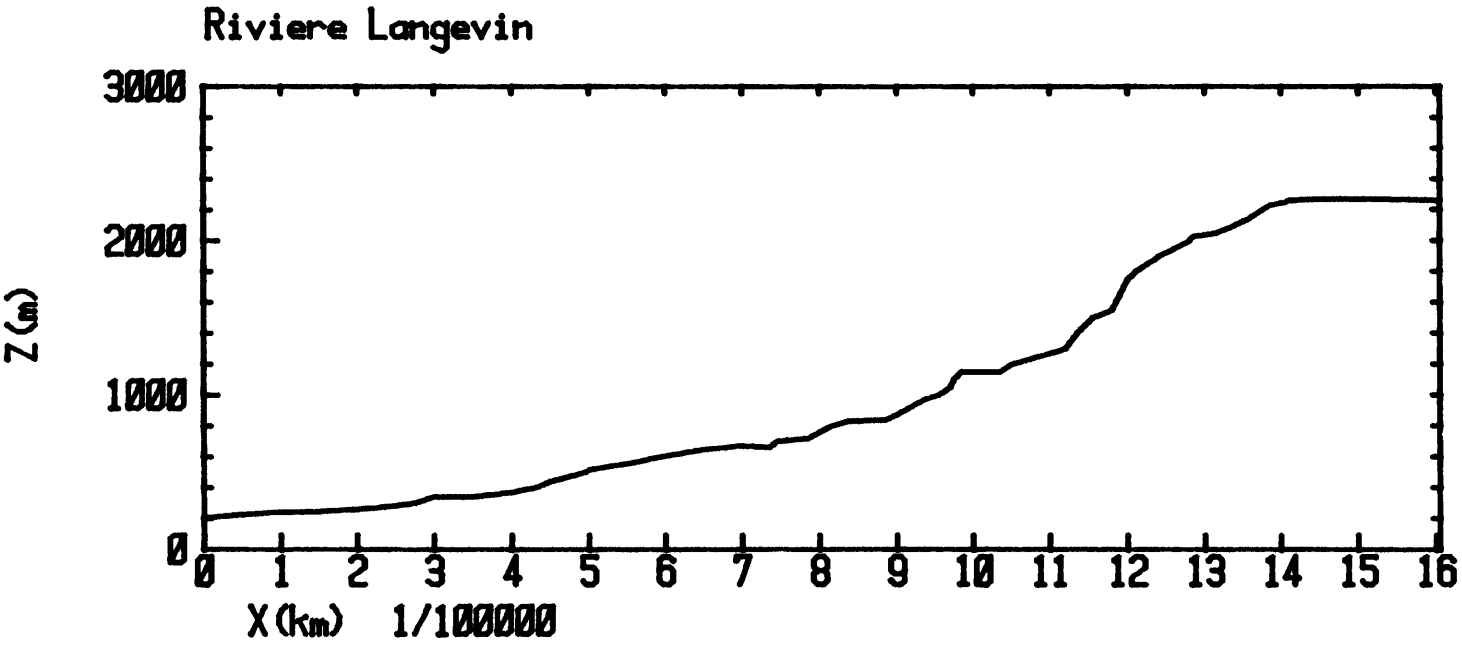

5. SP data and topographic profile from the Plaine des Sables. Data are unfiltered.

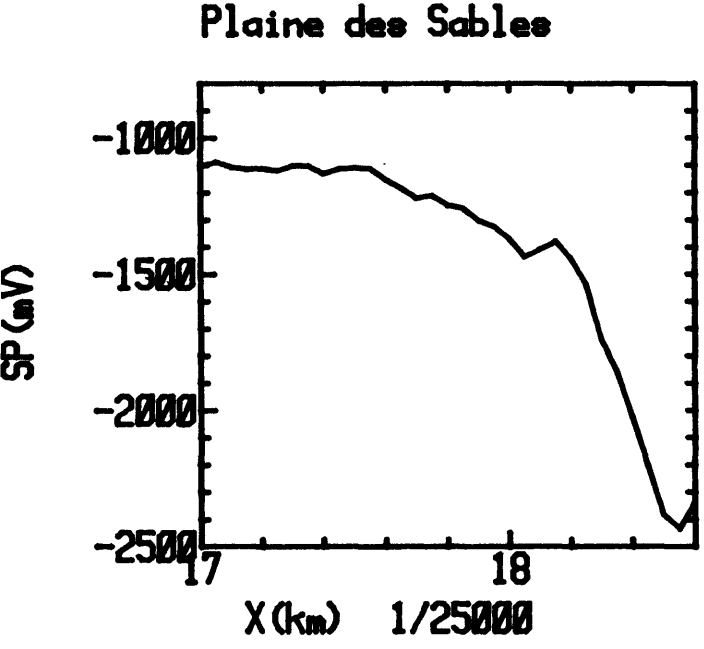

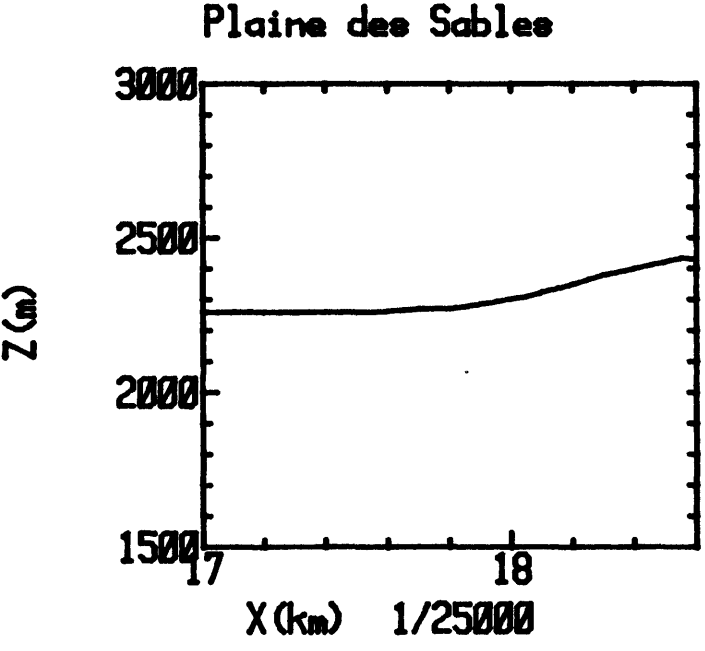

edge of the Plaine des Sables (14 km) to the region of Grand Pays (11 km) are normally dry except during torrential rains. However, farther south there is a continuous flow in the river, and springs are fairly common.

The reappearance of the river is explainable by two models. Moving southward down the Ravin de la Plaine des Sables we are moving stratigraphically lower in the geologic section. If there is an impermeable zone responsible for the horizontal waterflow and it crops out, the water will emerge from the ground at this level. Alternatively, if the impermeable zone does not crop out, but there is a localized impermeable region resting on the lower impermeable zone, a dam will be formed which causes the water to flow above ground. Geologically this localized impermeable zone might correspond to the zone of mudslide debris found in the area of Grand Pays and to the south. This material is probably less permeable than the indigenous basalt flows.

2.1.1 Division of data by anomaly (A) type

The data can be divided into two regions based on the type of anomaly. This separation is useful for the modelling of the data as different source types are envisioned for each region.

2.1.1.1 Anomalies associated with water flow (A1)

The anomalies on the Plaine des Sables and in the Ravin de la Plaine des Sables appear to be related to the flow of water. These regions are characterized by large amplitude anomalies (>500 mV) such as the large decrease in voltage (1300 mV) between 11 km and 14 km. Small scale features like the 100 mV anomaly near the 12 km point are superimposed on the regional anomaly. This is felt to be produced by a geologic feature, such as a dike, which the water flows past. This will be discussed in greater detail below.

2.1.1.2 Anomalies not associated with water flow (A2)

The region from 0 km to 11 km is characterized by several anomalies with amplitudes of less than 150 mV. This region is not considered to be as significantly influenced by subsurface water flow, because the river emerges near the 11 km point and continues to flow above ground. Thus streaming potential effects are diminished since the river can carry the preponderance of the runoff. There are two anomalies of major importance in this zone at a distance of 3 km and 10 km. A smaller anomaly of less significance is located at a distance of 7 km.

2.1.2 Division of data by correlation with topography (T)

The SP data can also be divided into regions where the correlation with elevation is linear. This type of relationship would be expected, if water was flowing through a vertical homogeneous column of rock. Figure 6 shows a plot of the data as a function of elevation. It has been divided into 6 segments. The table below gives the beginning and ending distance, the correlation with elevation and the equivalent streaming potential coefficient for each segment.

6. Plot of voltage versus elevation for the Rivière Langevin (A) and the Plaine des Sables (B).

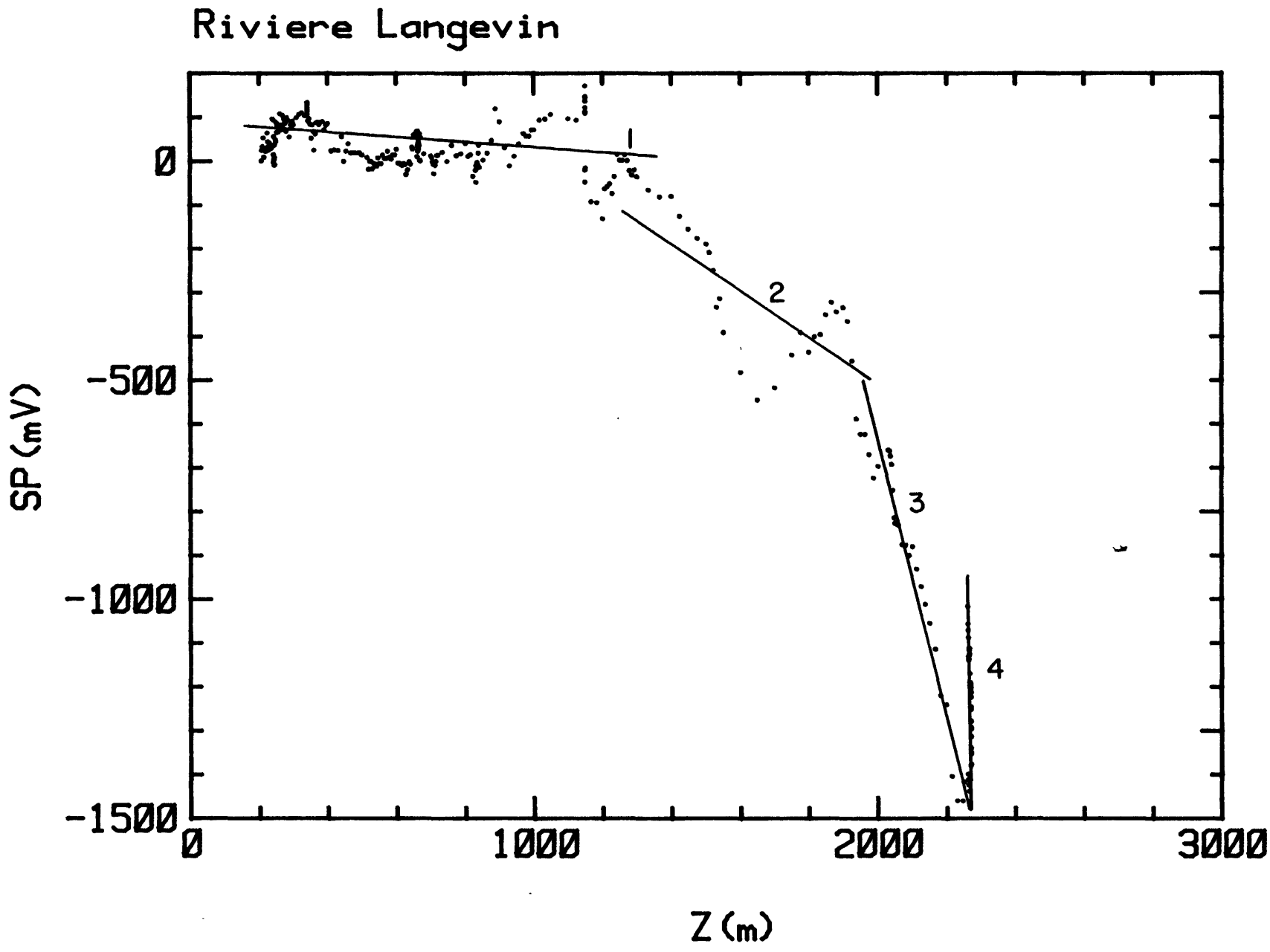

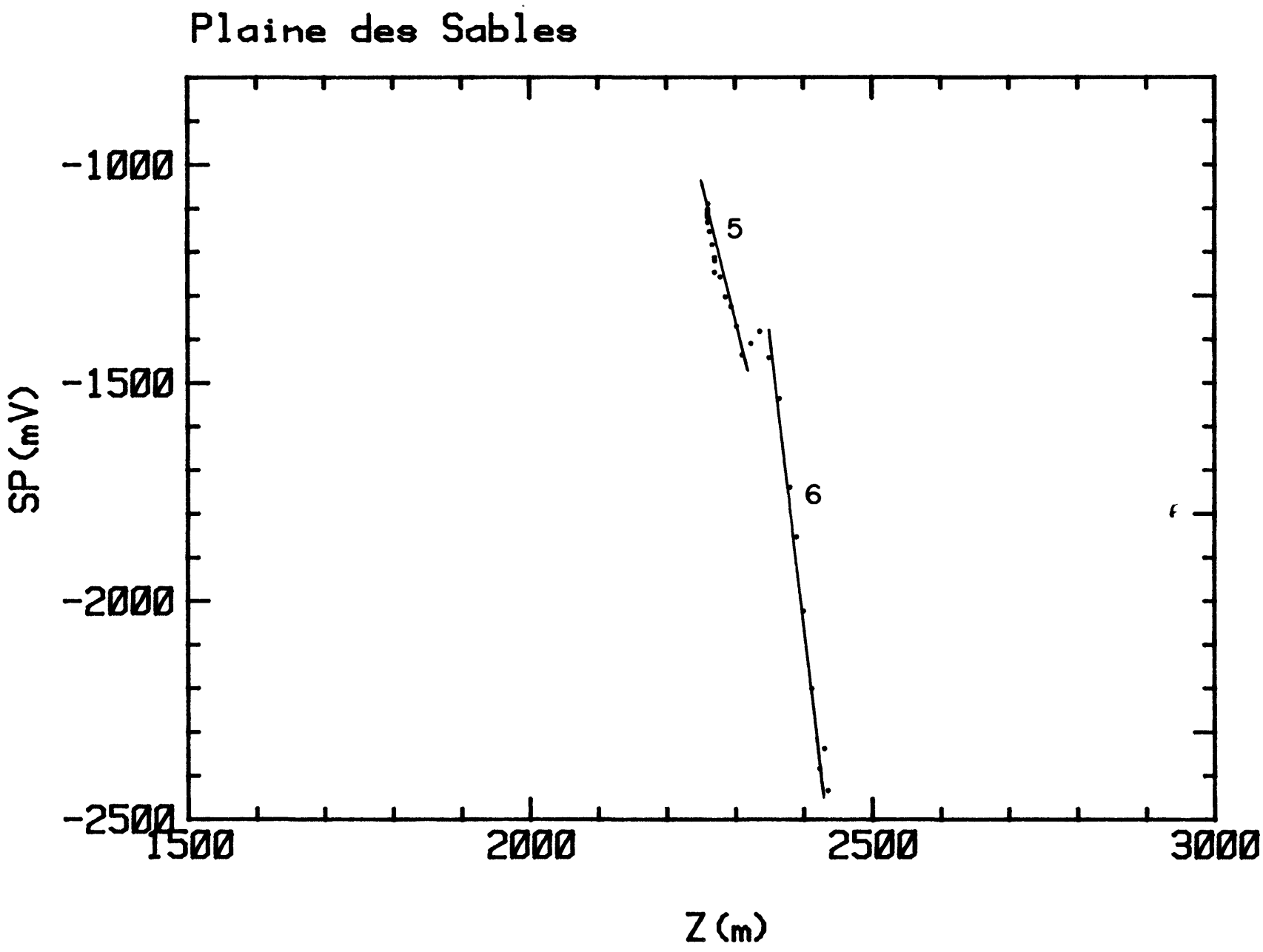
Plaine des Sables
-1000
-1500
-2000
-2500
SP (mV)
1500
2000
2500
3000
Z (m)
5
6

Table 1. Elevation correlation and equivalent streaming potential coefficient

Segment	Range (km)	mV/m	mV/bar[c]
1	0-11.40	-.064	.653
2	11.45-12.40	-.450	4.59
3	12.45-13.85	-2.81	28.7
4	14.00-16.05	+.021[b]	--
5[a]	14.30-15.35	-6.5	66.3
6[a]	15.40-15.95	-10.5	107

[a]These segments go across the Plaine des Sables from west to east

[b]Not well resolved

[c]1 mV/m ≃ 10.2 mV/bar

To obtain the equivalent streaming potential coefficient, it is assumed that there is a continuous column of water in the rock, and that the pressure increases 1 bar for each 10.2 m of elevation change. Estimates made this way are undoubtedly subject to some error as the pore spaces are not fully saturated. However, one can obtain relative values of the streaming potential coefficient for use in modelling.

It is interesting to note that the correlation of voltage with elevation increases in magnitude as the elevation increases. This observation supports the notion that the correlation is caused by a streaming potential mechanism. Streaming potential coefficients are inversely proportional to the pore fluid conductivity. The rain water which is the source of the flow is probably poorly conductive due to the lack of ions. As the water flows downward through the rocks it dissolves the rock, and the ion concentration and conductivity increase. This process leads to reduced streaming potential coefficients at lower elevations.

2.2 Interpretation of the anomalies

Two types of sources will be used to explain the SP anomalies. The first is the streaming potential effect, and the second is the thermoelectric effect. Streaming potential refers to electric currents produced by fluid flow through rocks, while the thermoelectric currents are driven by heat flow. Both mechanisms are caused by a difference in mobility between the positive and negative ions in the pore space. Near the pore wall the positive ion population is greater than the negative ion population, thus a force which induces ion migration, such as pressure or temperature gradients, will produce an enhancement of the positive ion population in the direction of fluid or heat flow. This motion of ions is called a convection current because it is produced by a charge which is carried by the primary flow. The resulting charge separation produces an electric field which drives a counter current called the conduction current. Based on the material properties and boundary conditions, different types of anomalies will be produced.

Mathematically, these two mechanisms can be described in a similar manner. The primary heat or fluid flow is described by a flow law

$$\vec{\Gamma} = - L_{11} \nabla \zeta \tag{3}$$

and a conservation law

$$\nabla \cdot \vec{\Gamma} = S \tag{4}$$

where ζ is temperature or pressure, L_{11} is thermal or hydraulic conductivity, $\vec{\Gamma}$ is heat or fluid flux, and S is a heat or fluid mass source. These equations with the appropriate boundary conditions can be solved to obtain ζ. The electric current is then described by

$$\vec{J} = -\sigma \nabla \phi - L_{12} \nabla \zeta \tag{5}$$

where ϕ is electric potential, σ is the electrical conductivity and L_{12} is a cross-conductivity. L_{12} should not be confused with the coupling coefficient

normally given by $C = L_{12}/\sigma$. The first term in equation (5) is the conduction current, and the second term is the convection current. Conservation of charge in the absence of sources requires that

$$\nabla \cdot \vec{J} = \nabla \cdot \vec{J}_{cond} + \nabla \cdot \vec{J}_{conv} = 0. \tag{6}$$

Rearranging equation (6) one realizes that the term $-\nabla \cdot \vec{J}_{conv}$ acts as a source for the measured electric potential ϕ.

$$\nabla \cdot \vec{J}_{cond} = -\nabla \cdot \vec{J}_{conv} = \nabla L_{12} \cdot \nabla \zeta + L_{12} \nabla^2 \zeta = \Sigma \tag{7}$$

The source term Σ is positive for positive current sources.

In this representation we can see that electric current sources exist where there are primary flows perpendicular to boundaries of the cross-conductivity L_{12}, and where there are divergences of temperature or pressure ($\nabla^2 \zeta \neq 0$) such as a pumping well or a hot body. Using these source descriptions, one can describe in a qualitative way the SP anomaly produced by a particular geometry and flow pattern. Quantitative modelling requires modelling the primary flow, calculating the electric current sources produced, and finally computing the electric potential. This procedure has been recently developed by Sill (1982). These ideas will be used only in a qualitative way to describe certain anomalies since we presently do not have access to a modelling program.

Another modelling approach is that first developed by Nourbehecht (1963) and used by Fitterman (1978, 1979) and Fitterman and Corwin (1982). A pseudo potential is defined

$$\psi = \phi + C\zeta \tag{8}$$

where ϕ is the measured electric potential, C is the coupling coefficient, and ζ is the temperature or pressure. The electric current is given by

$$\vec{J} = -\sigma \nabla \psi \tag{9}$$

Conservation of charge requires that

$$\nabla \cdot \vec{J} = -\sigma \nabla^2 \psi = 0 \qquad (10)$$

the sources of ψ can be shown to be

$$S = \Delta C \zeta \qquad (11)$$

that is differences of the coupling coefficient times the pressure or temperature. If ϕ is measured on a surface where $\zeta=0$, it has the same value as ψ.

The pseudo potential approach has the advantage that the primary field ζ need only be known on boundaries of C. This allows specifying ζ on boundaries of C without computing ζ everywhere in the half-space. There are, however, some definite drawbacks to the method. The condition of $\zeta=0$ on the surface of the half-space means that a vertical flux of $\vec{I}$ out of the half-space will exist. For the case of heat flow this is allowable, but for water flow this is not a reasonable boundary condition. Strictly speaking the approach is valid only for thermoelectric sources with the assumption that the surface of the half-space is at a constant temperature. The other problem with the pseudo potential formulation is that we really don't know the temperature field everywhere and how much heat input is required to maintain this temperature field. In principle we have specified enough information to compute the temperature field everywhere since it is only necessary to assume that the temperature goes to zero at infinity for the problem to be well-posed.

2.2.1 Interpretation of region A1 anomalies

This region is composed of the data on the Plaine des Sables (Figure 5) southward along the Rivière Langevin (Figure 4) to the 11 km mark. On the Plaine des Sables there are two profiles which cross each other at distances of 15.05 km on the north-south line (profile labeled Rivière Langevin) and

17.75 km on the east-west line (profile labelled Plaine des Sables). There are three significant features in the data. The first is the significant topographic effect on the Plaine des Sables profile as it climbs up Piton Chisny. The second is the topographic effect associated with the Rivière de la Plaine des Sables (11-13 km). This includes a smaller localized dipolar feature near the 12 km mark. The last is a negative monopolar anomaly near the south edge of the Plaine des Sables.

The flow of ground water from the high terrain near Piton Chisny toward the Plaine des Sables produces a negative anomaly by means of a streaming potential mechanism. A model of the source mechanism is shown in Figure 7. The fluid flows through a small block of rock. The downstream side of the rock becomes positive with respect to the other end because of charge accumulation. One can think of this model in terms of $\nabla L_{12} \cdot \nabla P$ sources. Assume ∇P is negative at both ends of the sample with the same amplitude, while ∇L_{12} is positive on the left end and negative on the right end. A convection current flows from the source on the right-hand side to the sink on the left-hand side. Because the conductivity is zero in the surrounding media, no current flows out of the block. The charge accumulation on the left-hand side produces an electric potential which drives a conduction current exactly equal to the convection current.

The situation on the Plaine des Sables is similar to this simple model. Water flow is driven by gravitational forces through the rock producing positive potentials in the direction of fluid flow. There is one component of flow downward from the high terrain near Piton Chisny. This produces the negative anomaly near the summit. Similar anomalies probably are associated with the summits of Piton de Hauy and Piton du Cirque which lie farther to the north.

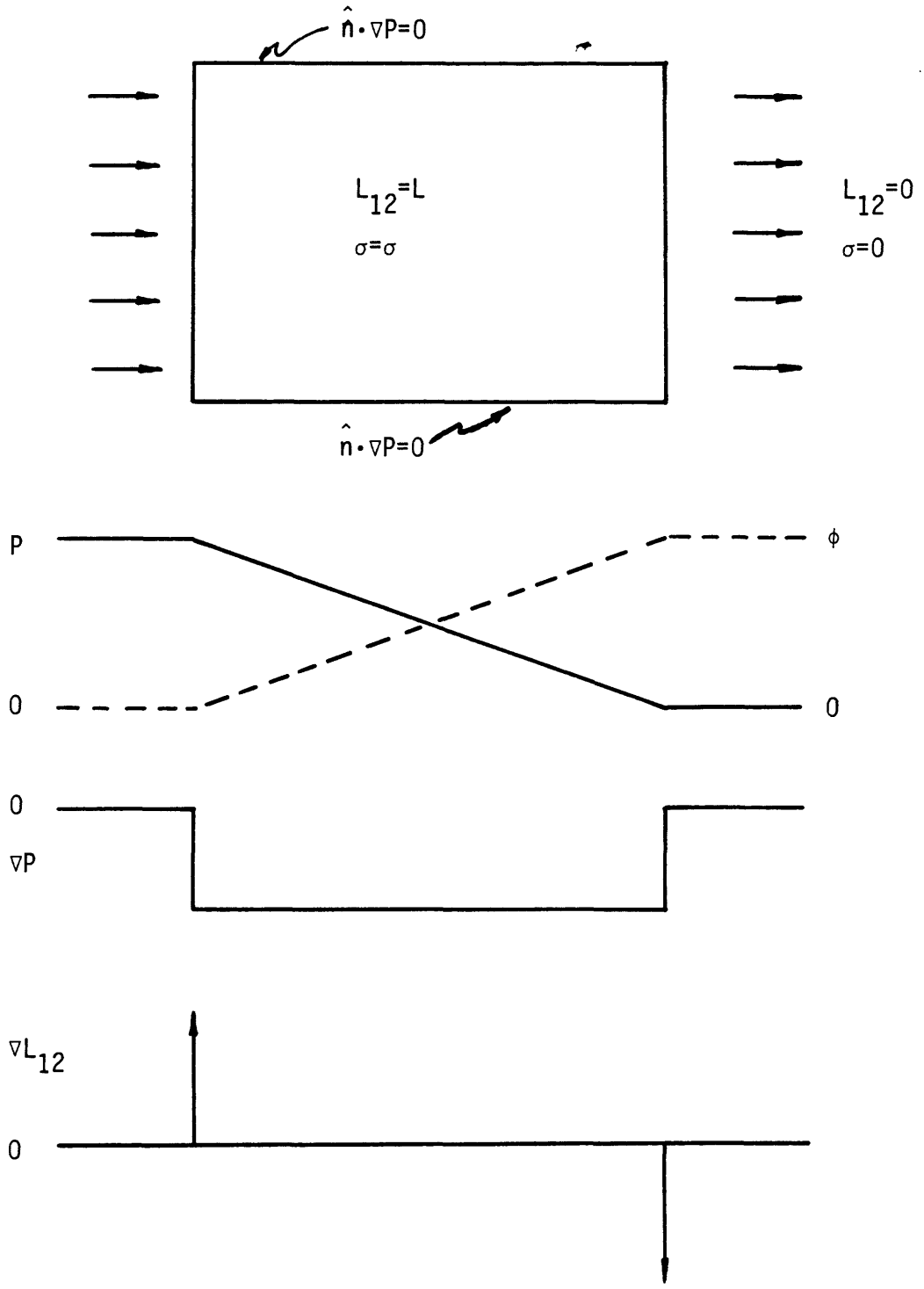

7. Model of SP source due to water flow in a homogeneous block.

A second topographic anomaly is seen on the Riviere Langevin profile (Figure 4) in the region 11-14 km. Geographically this region corresponds to the Ravin de la Plaine des Sables which descends from the Plaine des Sables about 1200 m to the Grand Pays. A large subsurface water flow probably exists in this region. The source of the flow is the almost daily rains on the Plaine des Sables and in the ravine. In the ravine, the drainages are normally dry, but farther south springs appear and the river flows. This overall flow accounts for the regional electrical anomaly gradient -- the downstream direction being positive (Figure 8). Superimposed on this there is a dipolar anomaly with a peak to trough amplitude of about 115 mV and a peak to trough length of about 400 m. This anomaly may be caused by a zone which modifies the flow regime. Geologically one envisions an intrusive feature such as a dike.

Two different models which explain the anomaly are presented in Figure 9. The first model (A) shows a dike with lower cross-conductivity parameter (L_{12}) than the host material. For simplicity it has been given a value of zero. A layer which also has an L_{12} value of zero covers the dike. This layer is not necessary for model A, but has been included to show the similarity with the second model. There is a regional flow from right to left which traverses the dike. This regional flow produces the large regional anomaly. The right-hand edge of the dike acts like a current source. This is caused by the $\nabla L_{12} \cdot \nabla P$ terms described in equation (7). Similarly on the left-hand edge of the dike a current sink is created. The effect of the two sources is to produce a dipolar shaped anomaly superimposed on the regional anomaly.

The second model (B) requires that the dike be of low permeability, and that there be an overlying layer with a smaller cross-conductivity than the

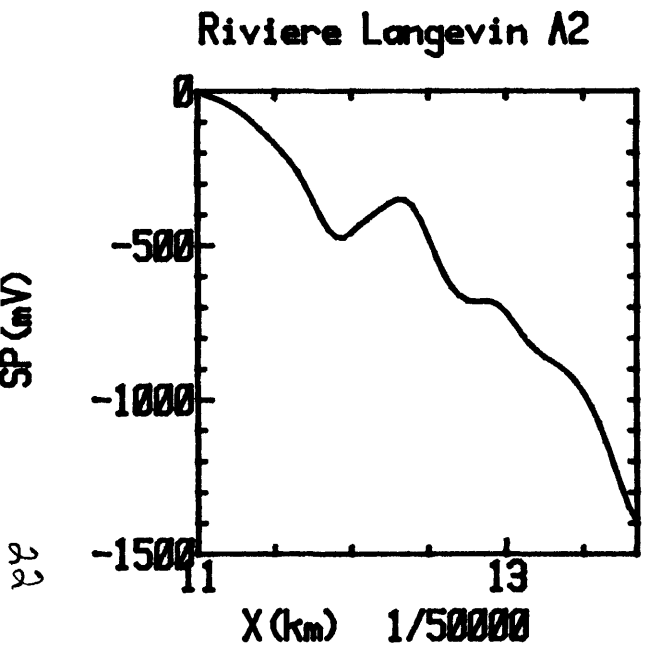

8. Region A2 SP anomaly from the Ravin de la Plaine des Sables.

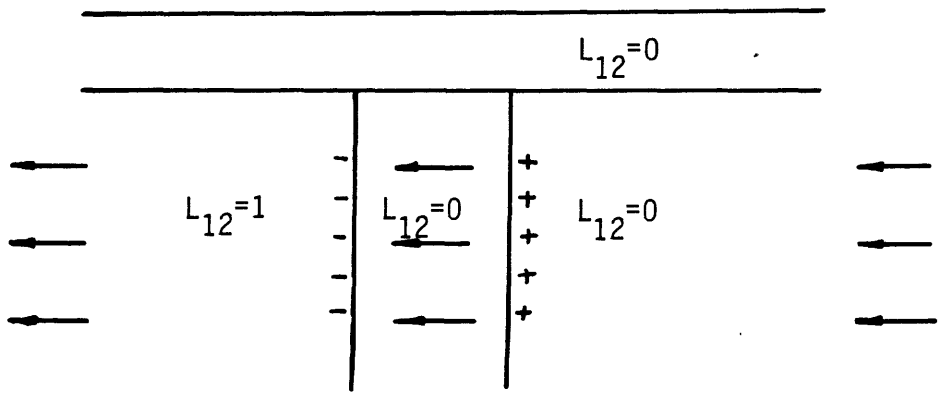

A. Permeable dike with lower streaming potential coefficient

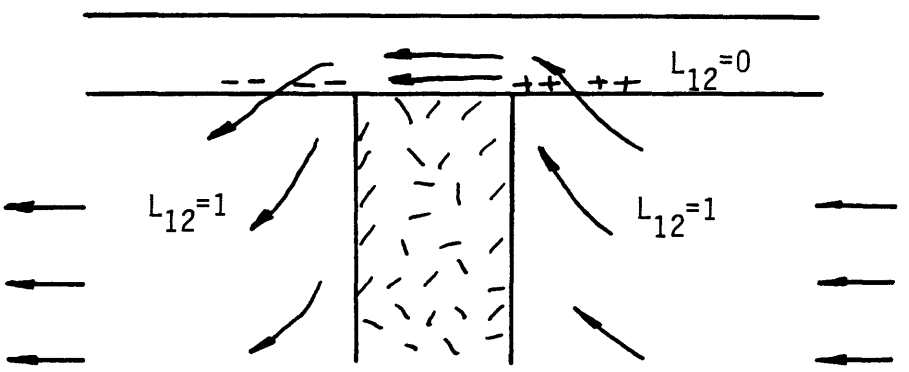

B. Low permeability dike overlain by low streaing potential coefficient layer.

9. **Models of fluid flow and charge accumulation caused by flow past permeable (A) and impermeable (B) dikes.**

host material. As the flow approaches the dike, it is forced upward into the more permeable overlying layer. After passing the impeding dike, the flow descends and resumes its regular flow. The low permeability dike is necessary to force the fluid flow to cross the cross-conductivity boundary and produce the current sources. The source is positive where the flow ascends and negative where it descends. The result is to produce an anomaly similar to that made by model A.

Without quantitative modelling we cannot tell if it is possible to differentiate between model A and B, nor can we say more about the exact geometry. It does apear, however, that the observed anomaly can be produced by an intrusive body. Geologically this is a feasible model as intrusions cutting across the lava flows are common. Furthermore, the horizontal interface required by model B is compatible with the observed volcanic structure, i.e., layer upon layer of lava flows.

The last feature of importance is the negative anomaly near the 14 km point. The increase of voltage to the south of this anomaly can be explained by water flow down the Ravin de la Plaine des Sables, but how can the voltage increase to the north be produced? A flow of ground water to the north could produce this increase, but hydrologically it is quite unlikely.

The key to understanding this anomaly comes from the dipole-dipole resistivity (DDR) data (Figure 10). The contours from DDR stations 8 to 2 slope near 45 degrees. This behavior is characteristic of a vertical contact. There is an opposite slope of the contours near stations 10 through 8. This behavior indicates a conductive feature between station 9 and 6, with resistive material on both sides. To the north under the Plaine des Sables the ground is more resistive than to the south of the conductor. The north edge of this conductor could produce the negative SP anomaly by creating a $\nabla L_{12} \cdot \nabla P$ source.

10. Dipole-dipole resistivity data for Rivière Langevin. Numbers above the horizontal axis refer to electrode numbers, while numbers below the axis gives approximate SP data kilometer marks.

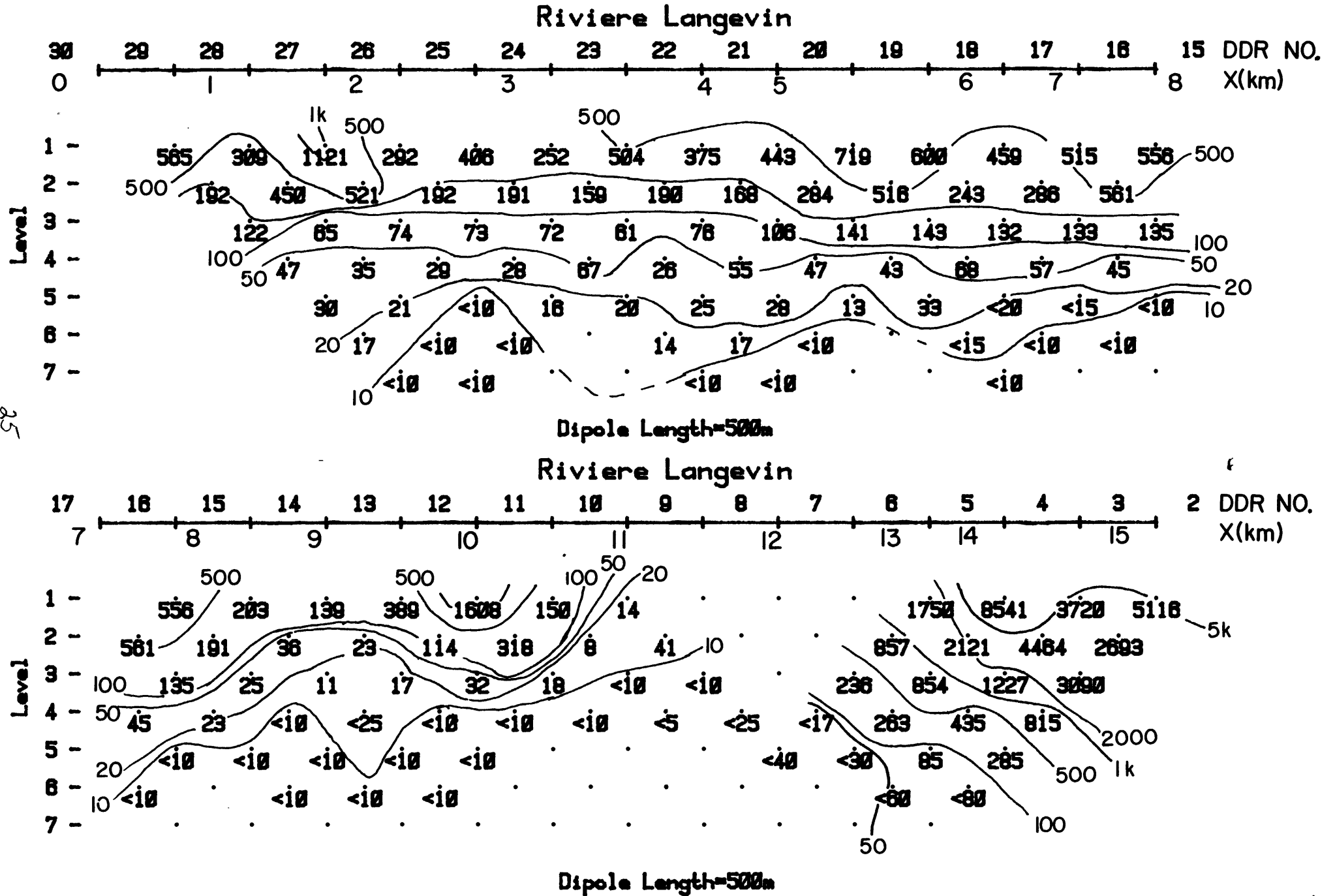

Consider a contact between two materials with different conductivity σ and, and different cross-conductivities L_{12} (Figure 11). (The streaming potential coefficients ($C=L_{12}/\sigma$) could be the same.) A flow of water exists from right to left. The source term $\nabla L_{12} \cdot \nabla P$ is non-zero only at the interface between the two materials, and is negative. Thus a current sink as discussed in Section 2.2 is present at the interface, producing a negatively charged region which gives rise to the negative SP anomaly. This source mechanism does not require that there be a streaming potential coefficient difference, only that the cross-conductivity ($L_{12}=\sigma C$) vary. Evidence for the conductivity changes comes from the DDR data which imples a change in cross-conductvity.

2.2.2 Interpretation of region A2 anomalies

The last zone, running from just north of Les Hirondelles to the south to the Grand Pays to the north, is the most interesting. This is a region where regional water flow is not considered to be of great significance. Because of this the interpretation was made using thermoelectric source models. This is not to say that streaming potential sources are not feasible, but having a means to model the anomalies with thermoelectric sources and in view of the reduced importance of fluid flow in this region, a thermoelectric source interpretation was chosen.

The profile which will be modelled is shown in Figure 12. An elevation correlation of -0.061 mV/m has been removed, and the data filtered with a 12 point running average. There are three anomalies of importance. The first centered near the 3 km point, the second near 7 km, and the third near 10 km. Initially it was felt the anomalies might be caused by a dike like or rift structure located between the 3 km and 10 km anomalies. This model was suggested by other electrical data. High-frequency magnetotelluric (AMT) measurements have located a conductive zone between distances 5.6 km and

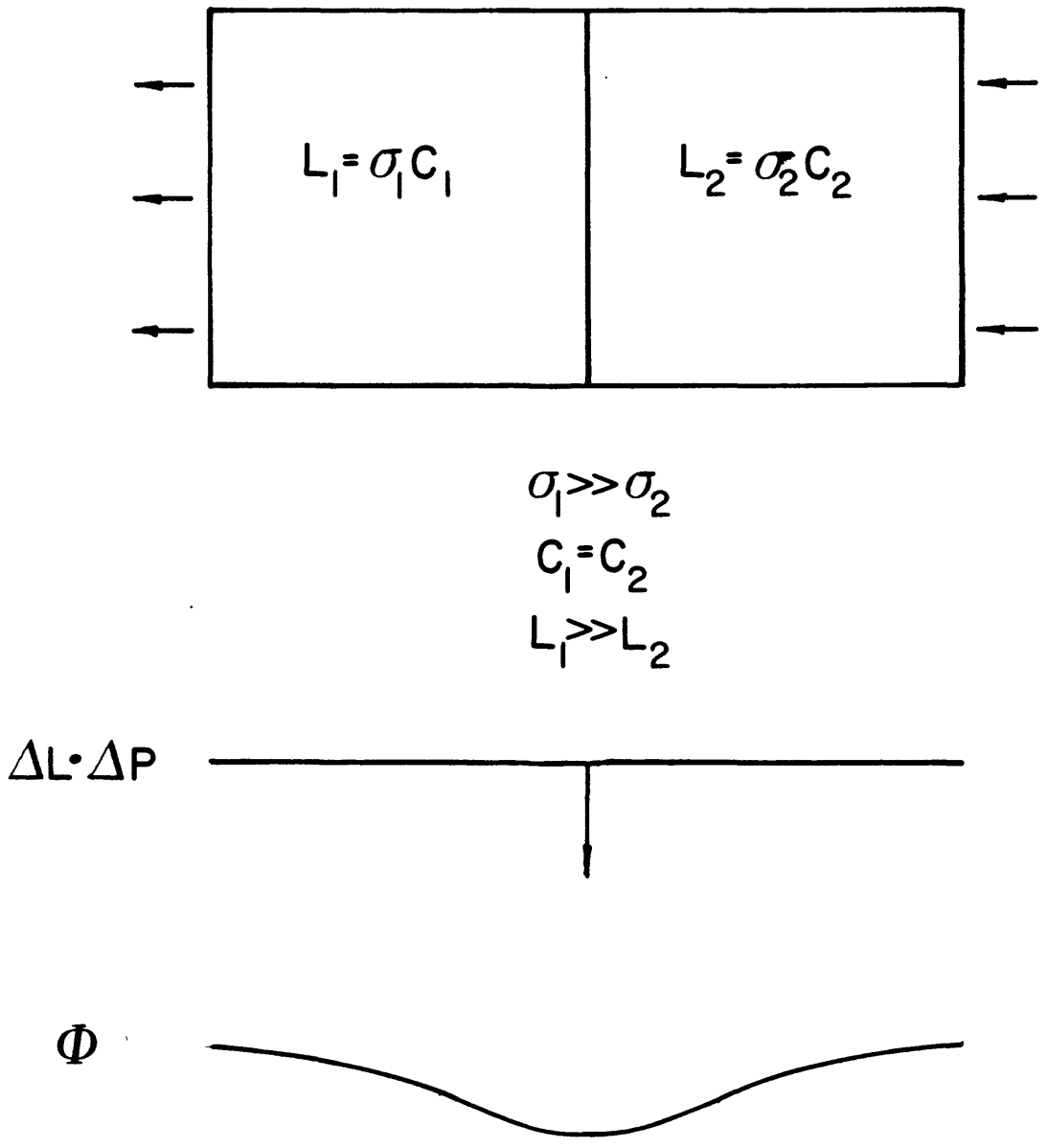

11. Model of flow across conductivity boundary producing a negative monopolar SP anomaly.

12. Region A2 SP anomaly from the Rivière Langevin. An elevation correlation of -0.061 mV/m has been removed. Data are filtered with a filter length of 12.

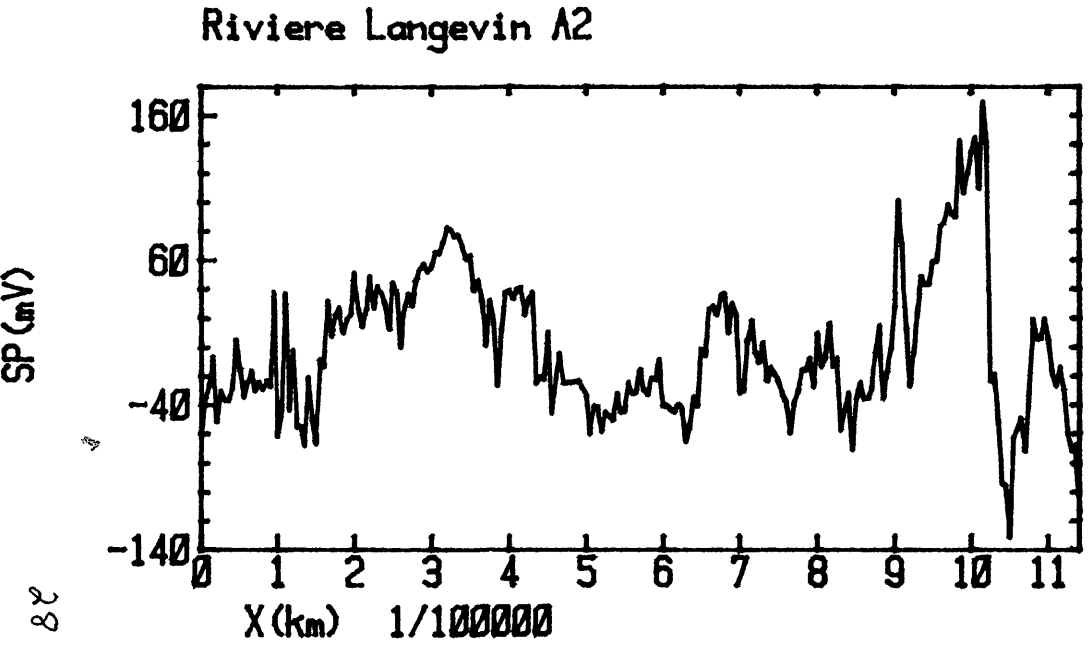

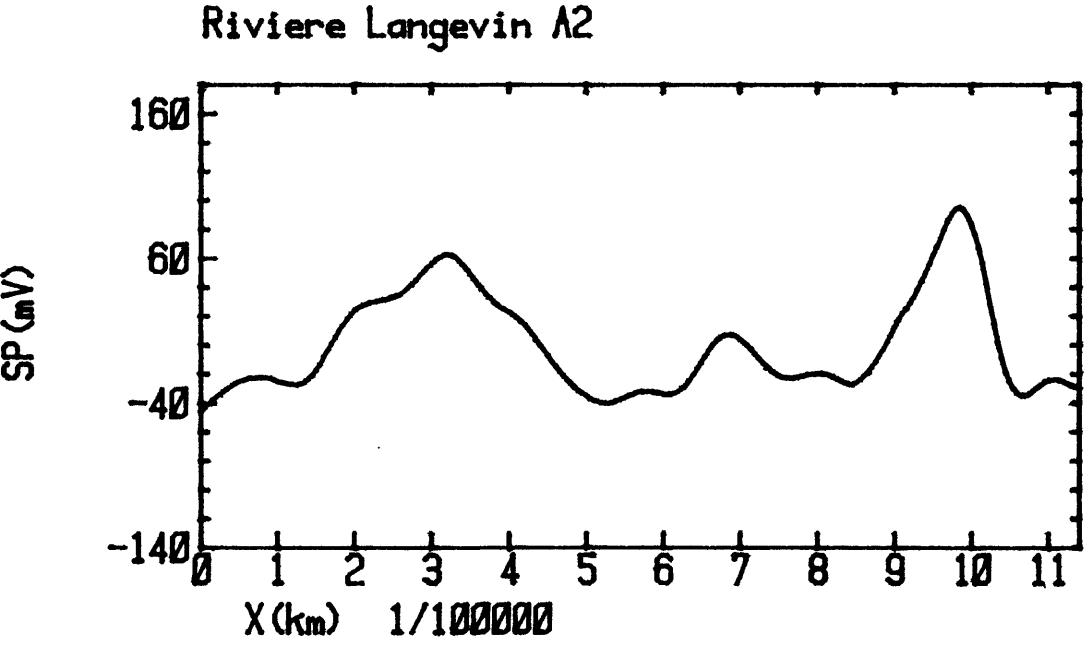

9.35 km (Benderitter and Gérard, 1981). This zone is about five times more conductive than the adjacent regions. The zone has a resistivity of about 100 Ωm at high frequencies (80-1700 hz) and a resistivity of 30 Ωm at low frequencies (8-80 hz). The interpreted depth to the top of the conductor varies from 300 m to 500 m. The region to the north of the conductive zone shows apparent resistivities of 500 Ωm at high frequencies, diminishing to 50 Ωm at low frequencies, and the conductor tends to be deeper (600 m). To the south there is a similar picture; a resistive first layer (300 Ωm) is underlain by a conductive zone (50 Ωm - 100 Ωm) at a depth of about 500 m to 700 m. In general there is an upwelling of the conductivity zone in this region.

The results of a vertical rift zone (dike) SP model with homogeneous conductivity are shown in Figure 13. The source is caused by a thermoelectric mechanism with the edges of the rift being at an elevated temperature, and the surrounding material having larger thermoelectric coupling coefficients than the rift. Thus the flow of heat away from the rift makes it more negative than the surrounding material. The sources are polarized rectangular plates with length ℓ, vertical dimension t, and depth to top d. The intensity of the source F is determined by the difference in thermoelectric coefficients times the temperature. Source 1 is polarized positive to the left and source 2 is polarized positive to the right. The location of the sources is shown below the anomaly. The arrow on each source plate shows the direction of positive polarization.

The length of all sources has been fixed at 2 km. This length was chosen because it is compatible with the width of the valley. Since the SP data was only gathered along a profile, we have no way of determining the source length.

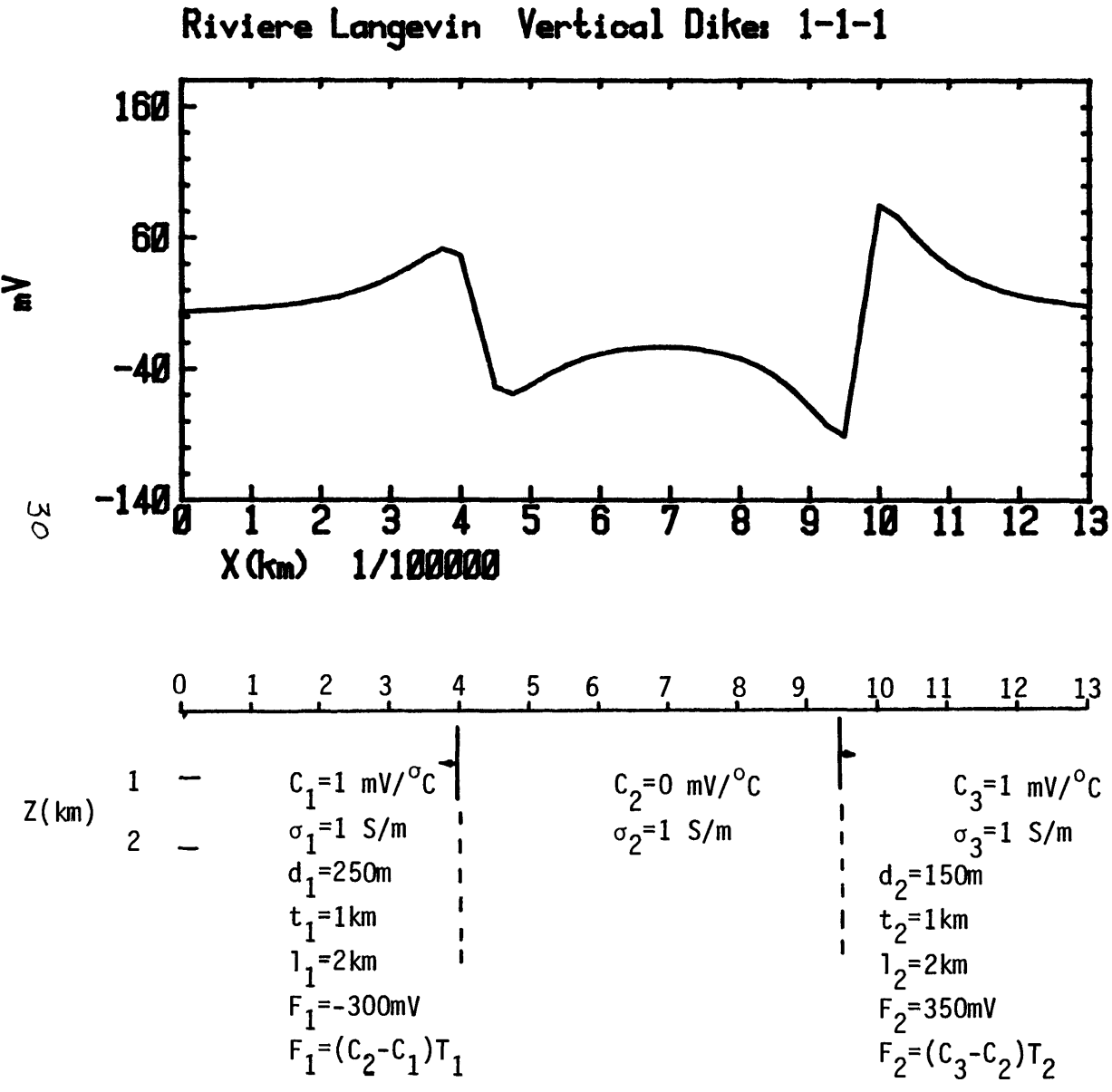

13. Vertical dike SP anomaly with homogeneous conductivity.

The anomaly produced by this source geometry shows a vague resemblance to the data (Figure 12) in that there are two positive features. The rapid decrease in potential to the north and south of these two features is not observed in the model profile. The small 7 km anomaly is also missing, but it is not modellable with this simplified geometry. Making the rift zone five times more conductive (Figure 14) flattens the anomaly over the rift zone and increases the slope of the anomaly outside of the rift zone. However, the slope of the measured data is steeper on the north side of the anomaly than on the south side. This type of behavior is not possible with vertical dike models, nor is it possible to have the same slope on both sides of a source with this geometry.

We now look at an interpretation using rectangular source planes which are free to have their orientation changed. This freedom is gained at a price, namely that we are limited to a homogeneously conductive medium. This is at odds with dipole-dipole resistivity data which indicates lateral and vertical conductivity variations. Figure 15 shows a model which fits the data. The length of the sources were kept constant at 2 km, and the source strengths were kept below 350 mV. One should also remember that SP data inversion is by no means unique, thus several models can exist which produce the same geometry. The model results correspond well with the 3 km and 10 km observed anomalies except for a bias of about 40 mV. Bias differences are not significant as potential measurements are always relative to an arbitrary reference point. While no attempt was made to model the small anomaly at 7 km, it could be modelled with a source polarized in the same sense as the 3 km and 10 km sources. The source planes represent a boundary across which the thermoelectric coupling coefficient changes, and is polarized by elevated temperature.

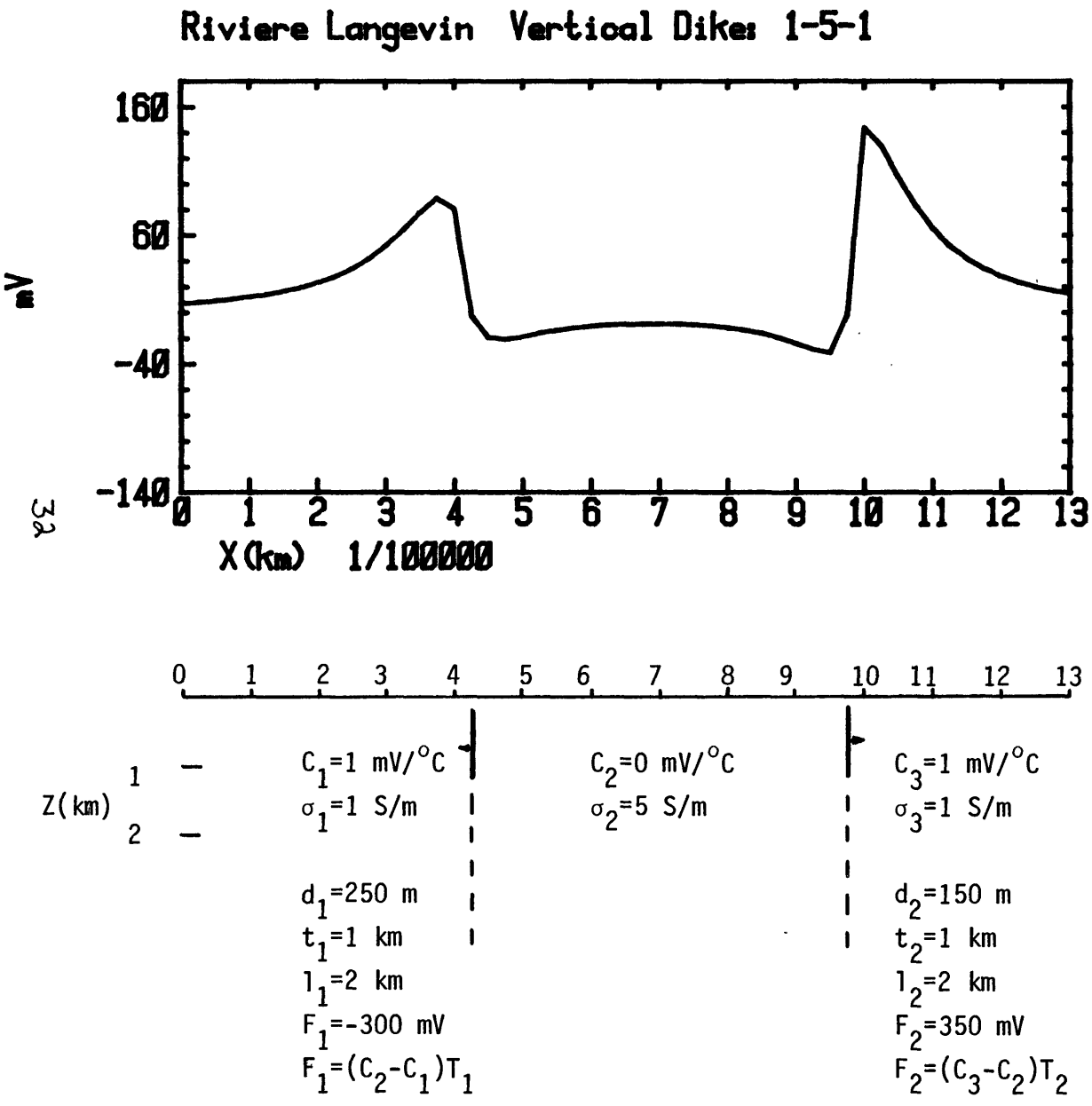

14. Conductive vertical dike SP anomaly.

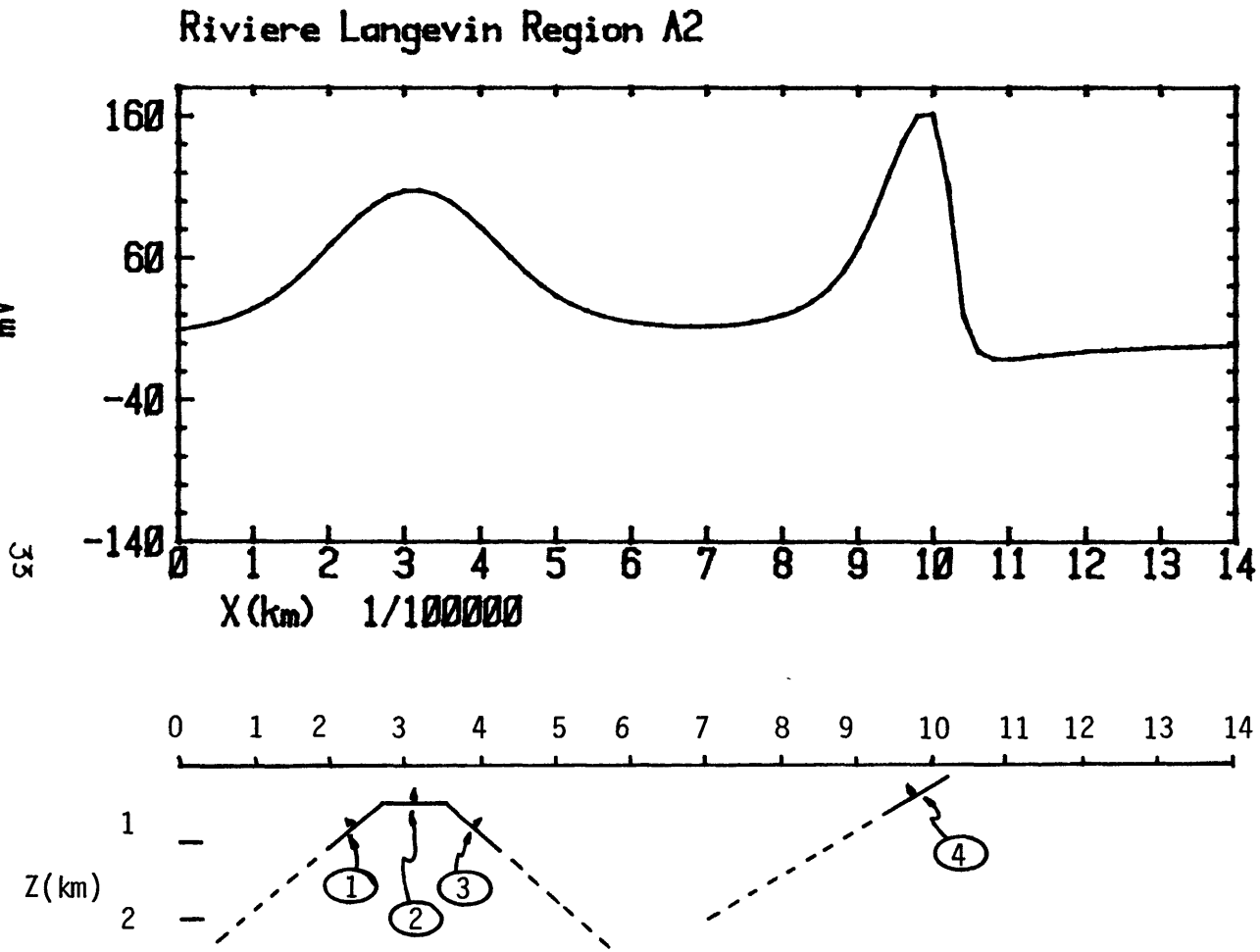

Source	d(m)	t(km)	l(km)	F(mV)	dip(°)
1	500	1.00	2.00	250	40
2	500	0.75	2.00	250	0
3	500	1.00	2.00	250	40
4	150	1.00	2.00	300	30

15. Thermoelectric source model of region A2 SP anomaly. (A) SP anomaly and vertical location of sources. (B) Map view source and traverse locations. (C) SP anomaly at same scale as DDR data.

Riviere Langevin Region A2

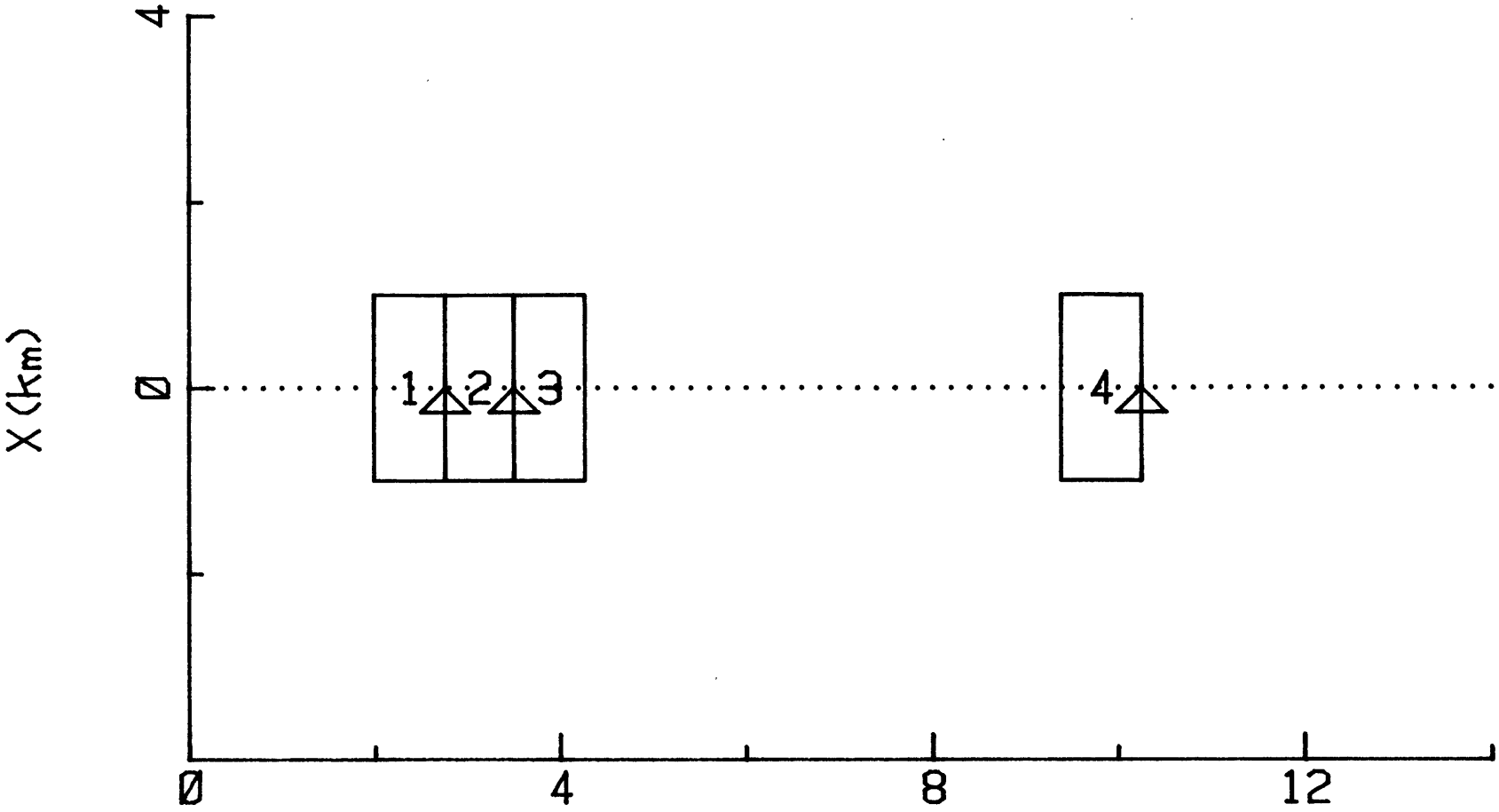

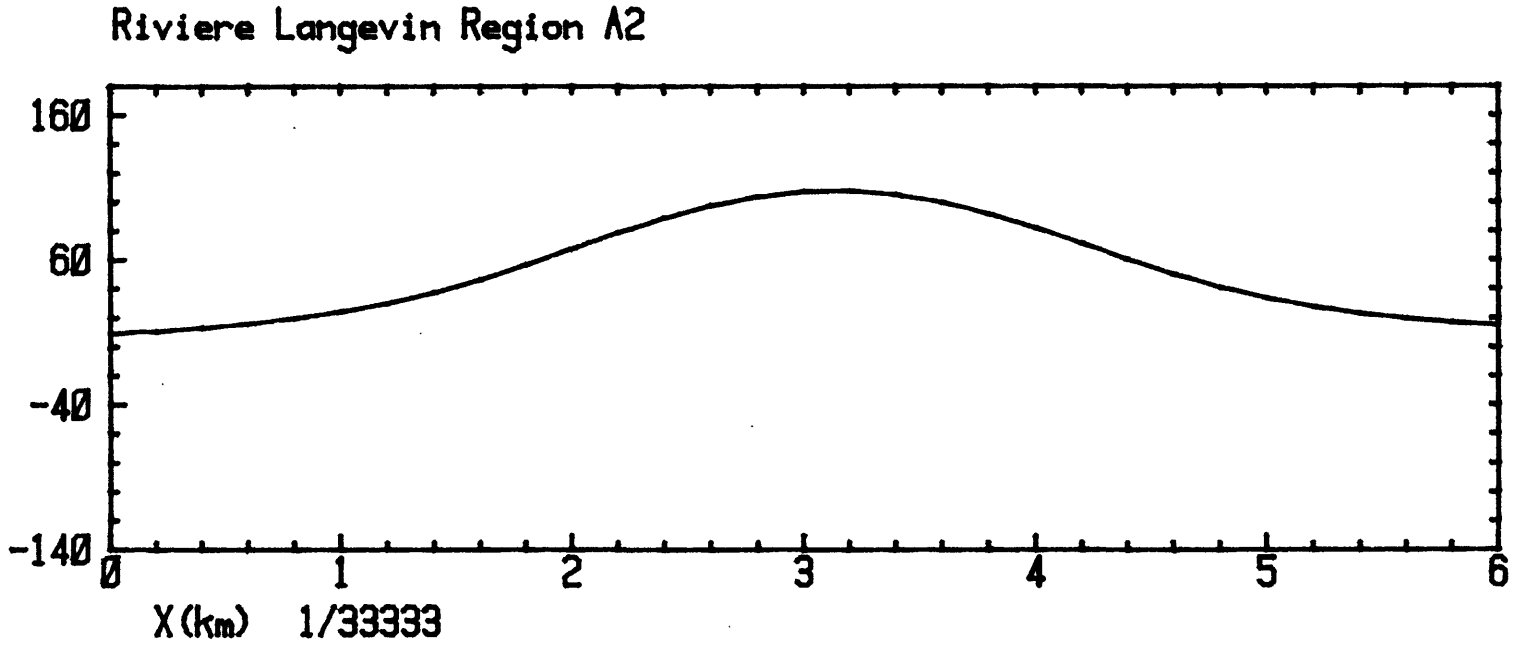
Riviere Langevin Region A2
160
60
-40
-140
mV
0
1
2
3
4
5
6
X(km) 1/33333

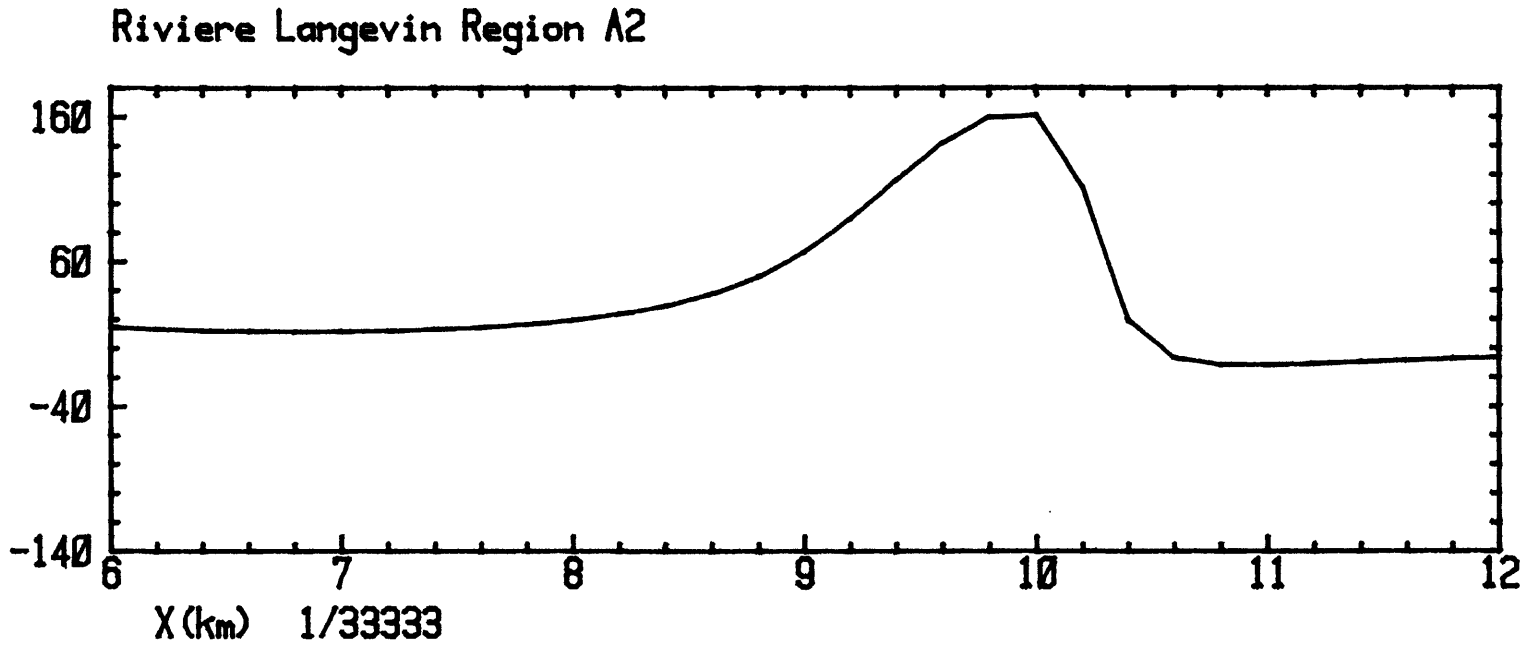
Riviere Langevin Region A2
160
60
-40
-140
mV
6
7
8
9
10
11
12
X(km) 1/33333

The 3 km anomaly is modelled with three source patches which form a roof shaped structure. The depth to the top of this feature is 500 m, with two side planes dipping at 40°. A source intensity of 250 mV has been used. The 10 km source is shallower (150 m) and has a slightly greater intensity than the other sources.

The source locations correspond with zones of increased conductivity in the dipole-dipole resistivity (DDR) data (Figure 10). The 3 km anomaly corresponds to the conductive bump seen between DDR stations 24 and 25. Similarly the 10 km SP source corresponds with the conductivity boundary seen between resistivity stations 10 and 14. The depth of the SP sources is in general agreement with the interpreted depth to the conductor. The boundary between the conductive material below and the resistive near surface material could produce the thermoelectric boundary required by the model. The conductor probably corresponds to the zeolitized basalt lava which underlies the phase 3 and phase 4 formations of Piton de la Fournaise (Billard, 1974). In regions of elevated temperature this interface could act as an SP source.

2.3 Summary of results

The following results in decreasing order of exploration importance can be drawn from the data:

1. In region A2, the anomalies at 3 km and 10 km correspond with observed resistivity lows at depth. They are interpretable as being caused by a thermoelectric source mechanism associated with a boundary of thermoelectric coupling properties and elevated temperature. The correspondence between the conductors and the SP anomalies makes them interesting geothermal targets.
2. The large negative anomaly associated with Piton Chisny is the result of water percolation toward the Plaine des Sables.

3. Water flow down the Ravin de la Plaine des Sables produces a topographic effect. Superimposed on this feature is a small anomaly near the 12 km mark which could be produced by an intrusive feature, such as a dike, with different cross-conductivity properties than the surrounding rock.

4. The negative anomaly at the south edge of the Plaine des Sables is produced by water flow across a conductivity boundary.

3. Cirque de Salazie

Two SP profiles were made in the Cirque de Salazie. The first profile goes from Ilet Morin through the villages of Salazie and Hell-Bourg toward Ilet à Vidot. The second profile goes from Salazie village towards Grand Ilet. The two profiles will be referred to as "Hell-Bourg" and "Grand Ilet" respectively.

Dipole-dipole resistivity (DDR) measurements were made along an adjacent route by a B.R.G.M. crew. Figure 16 shows the locations of the SP and DDR measurements.

3.1 Treatment of the data

These data required different treatment than the data from the Rivière Langevin primarily because of the tortuous profile. The raw data are shown in Figure 17. Several points which were considered spurious because of their short wavelength and large amplitude (marked by diamonds) were replaced by linearly interpolating between neighboring points. The data were then adjusted for topographic effects. A topographic correction of 0.169 mV/m was used on the Hell-Bourg profile, and 0.163 mV/m on all but the last 2.35 km of the Grand Ilet profile. An 8 point bi-directional running average filter was applied to the data to reduce noise.

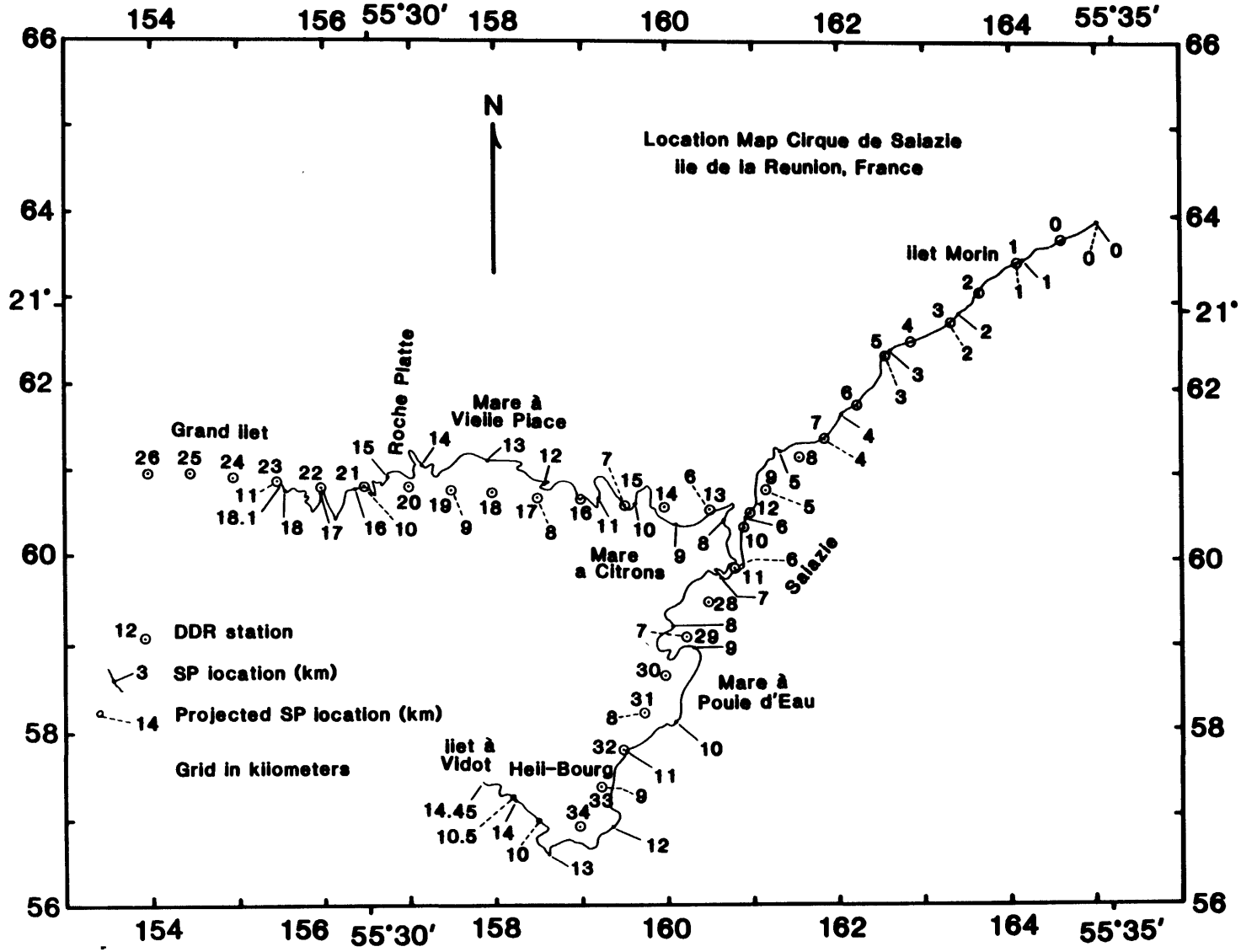

16. Location map of SP and DDR traverses in the Cirque de Salazie. The horizontal and vertical scales are in kilometers and refer to the scales in Figure 2.

17. Raw SP data from the Cirque de Salazie. The circled data points have been removed.

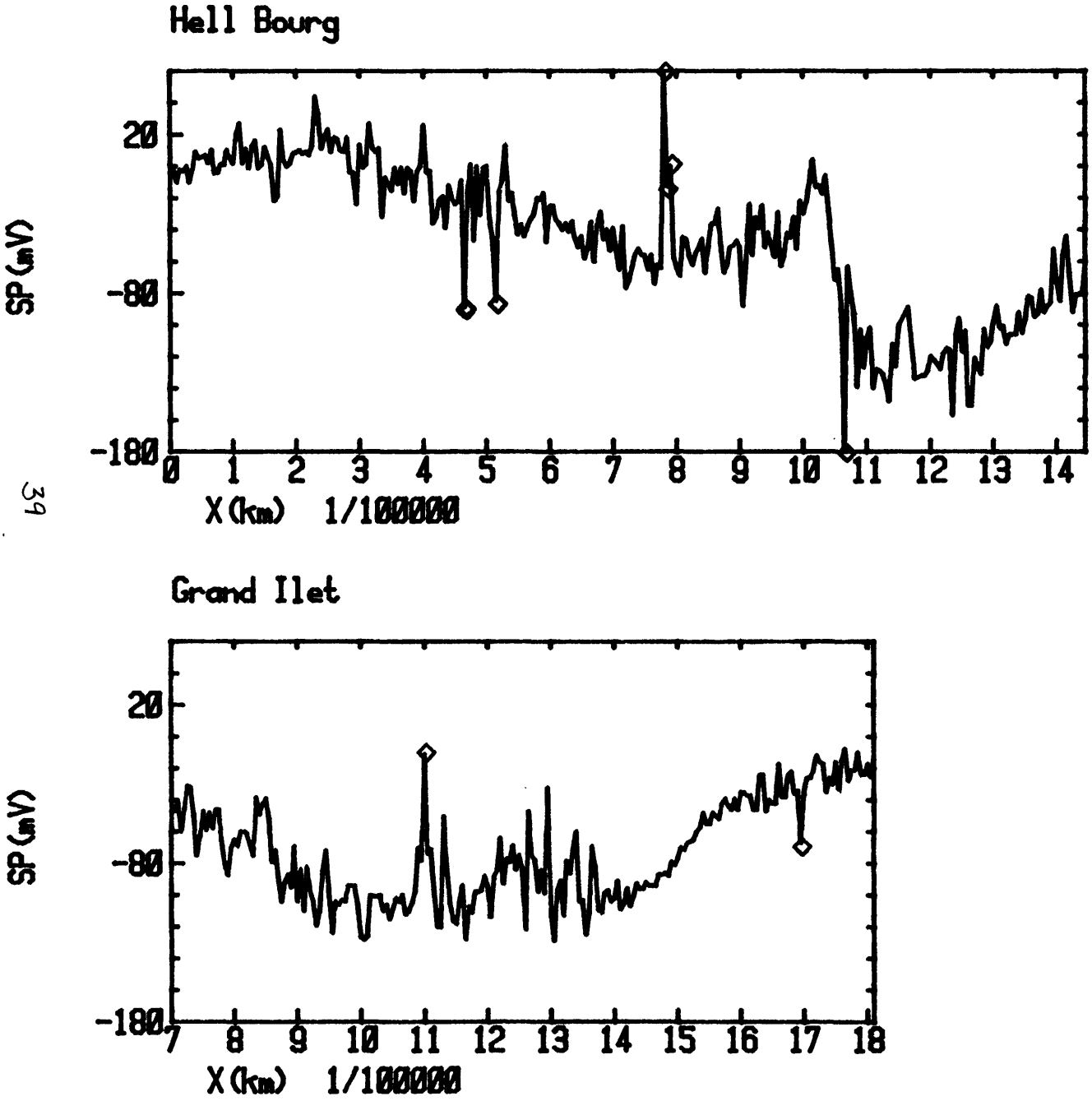

For ease of interpretation and comparison with the DDR data, the SP data were projected onto the measurement line of the DDR data. The projected profiles are shown in Figures 18 and 19 along with the DDR data.

3.2 General characteristics of the SP data

The Hell-Bourg profile shows a broad peak of about 40 mV centered near distance 2 km. The potential decreases to a minimum located at 6.5 km with an amplitude of -30 mV. A very pronounced anomaly is located near 8 km exhibiting a sharp positive peak of about 50 mV and a trough of about -30 mV. The potential then increases steadily to the end of the profile.

The Grand Ilet profile, which joins the Hell-Bourg profile near 5.5 km, has a broad negative of -50 mV near 6.8 km. The anomaly flattens in the region of 8.5 km near the zero level before dropping slightly to -20 mV. After this minimum at 9.4 km the anomaly increases steadily in a manner similar to the Hell-Bourg profile.

3.3 Comparison of SP anomalies with DDR data

The conductivity structure of the Hell-Bourg profile is dominated by a conductive zone between stations 7 and 31. The pronounced SP anomaly with a peak near 8 km corresponds with the south-west boundary of the conductor. Using a single inclined thermoelectric source, this anomaly can be modelled with moderate success (Figure 20). The interface between the different thermoelectric materials dips at 60^{o} to the north-east. The top of the rectangular source is at a depth of 100 m with a dip length of 500 m and a strike length of 1.5 km. The source intensity of 175 mV is assumed to be produced by an elevated temperature near the interface. The material to the northeast of the source plane is assumed to have a greater thermoelectric coefficient than the material on the other side of the source plane.

18. Projected SP and DDR data for Hell-Bourg traverse. A topographic correlation of -0.169 mV/m has been removed, and the data filtered with an 8 point bi-directional running average.

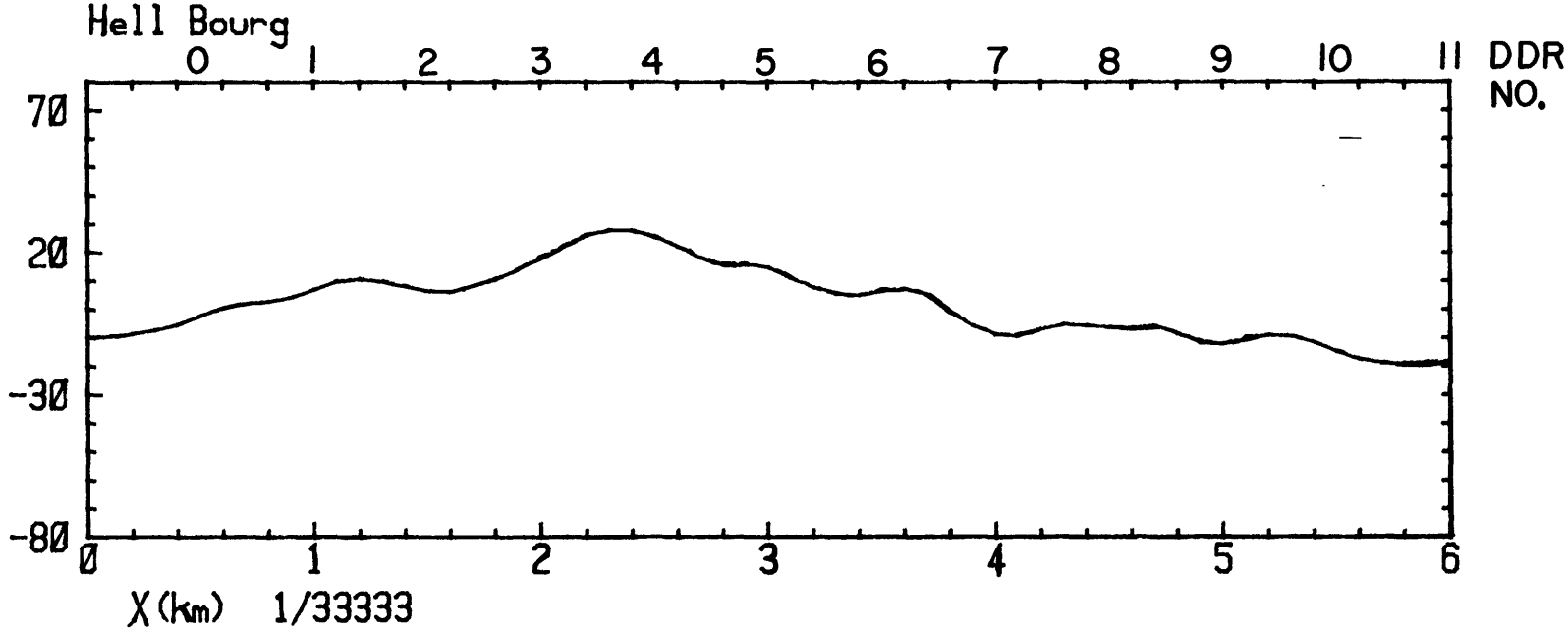

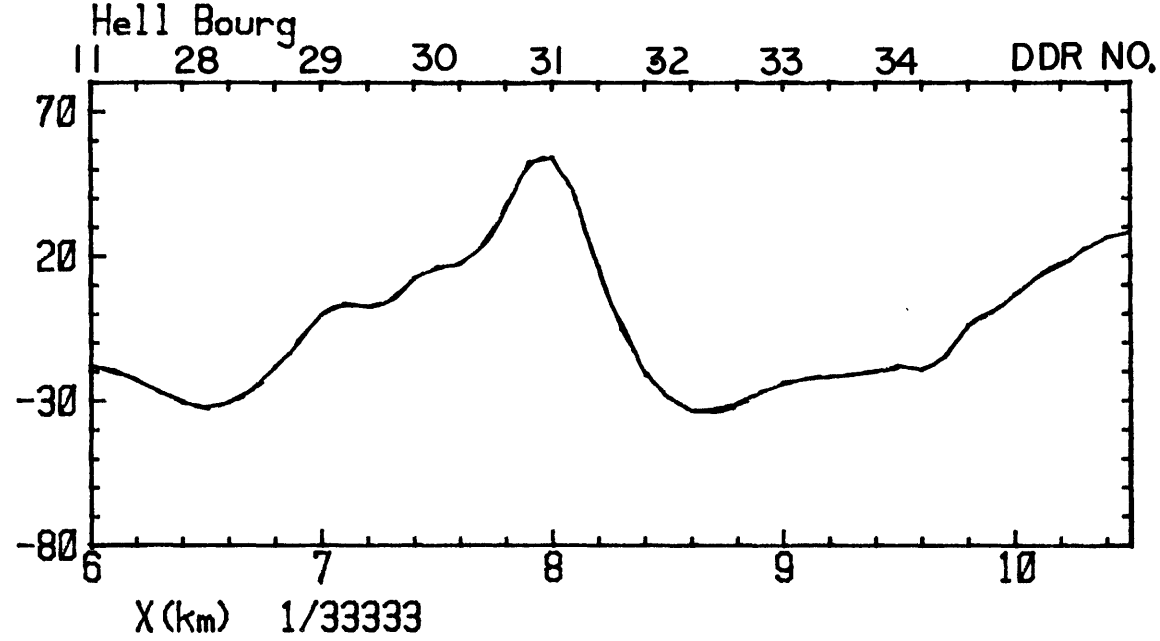

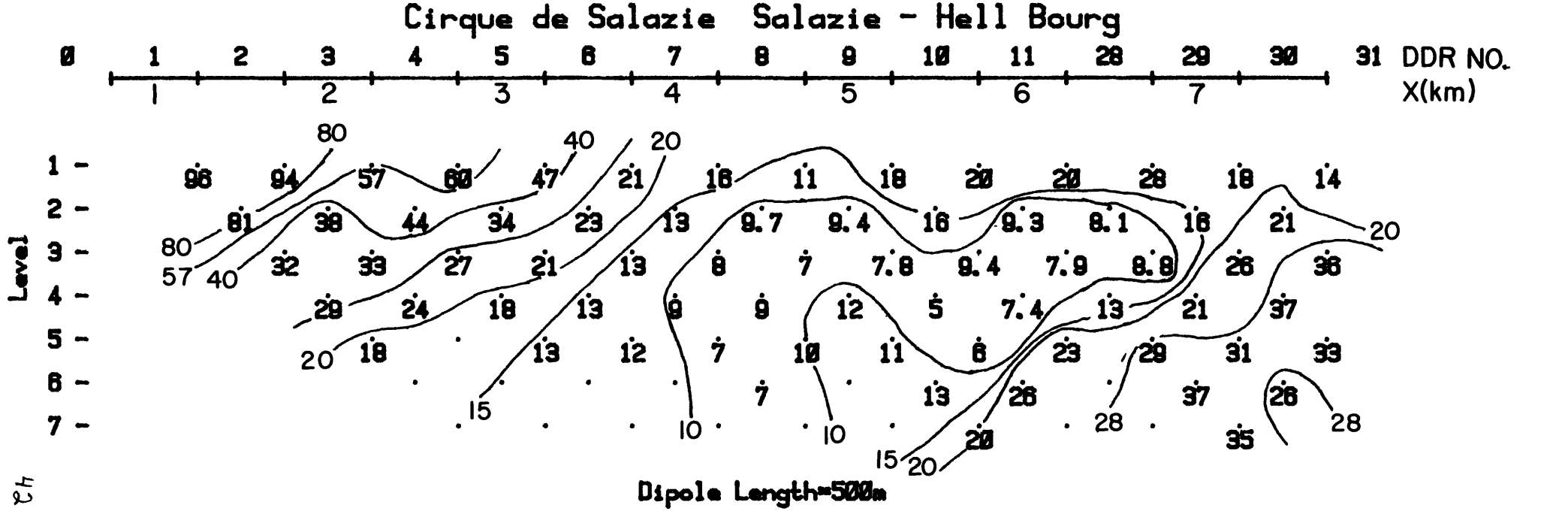
Cirque de Salazie Salazie - Hell Bourg
0 1 2 3 4 5 6 7 8 9 10 11 28 29 30 31 DDR NO.
1 2 3 4 5 6 7 X(km)
Level
1 2 3 4 5 6 7
80 40 20
96 94 57 60 47 21 16 11 18 20 20 28 18 14
81 38 44 34 23 13 9.7 9.4 16 9.3 8.1 16 21 20
80 57 40 32 33 27 21 13 8 7 7.8 9.4 7.9 8.8 26 36
29 24 18 13 9 9 12 5 7.4 13 21 37
20 18 13 12 7 10 11 6 23 29 31 33
15 7 13 26 37 26 28
10 10 28
15 20 20 35
Dipole Length=500m

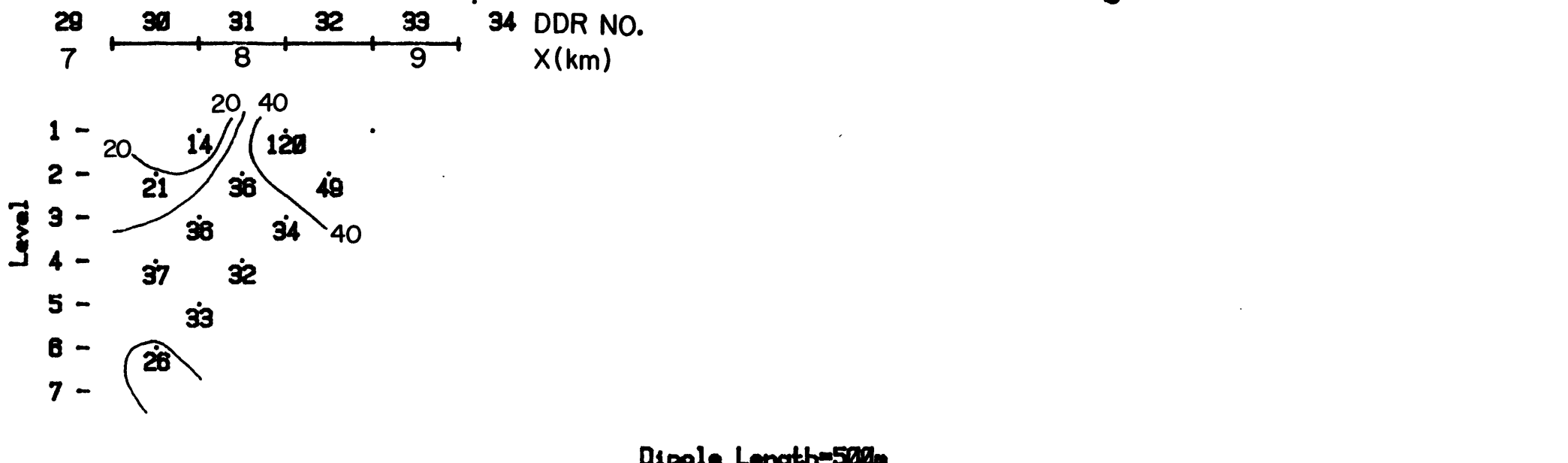
Cirque de Salazie Salazie - Hell Bourg
29 30 31 32 33 34 DDR NO.
7 8 9 X(km)
Level
1 2 3 4 5 6 7
20 40
20 14 120
21 36 49
36 34 40
37 32
33
26
Dipole Length=500m

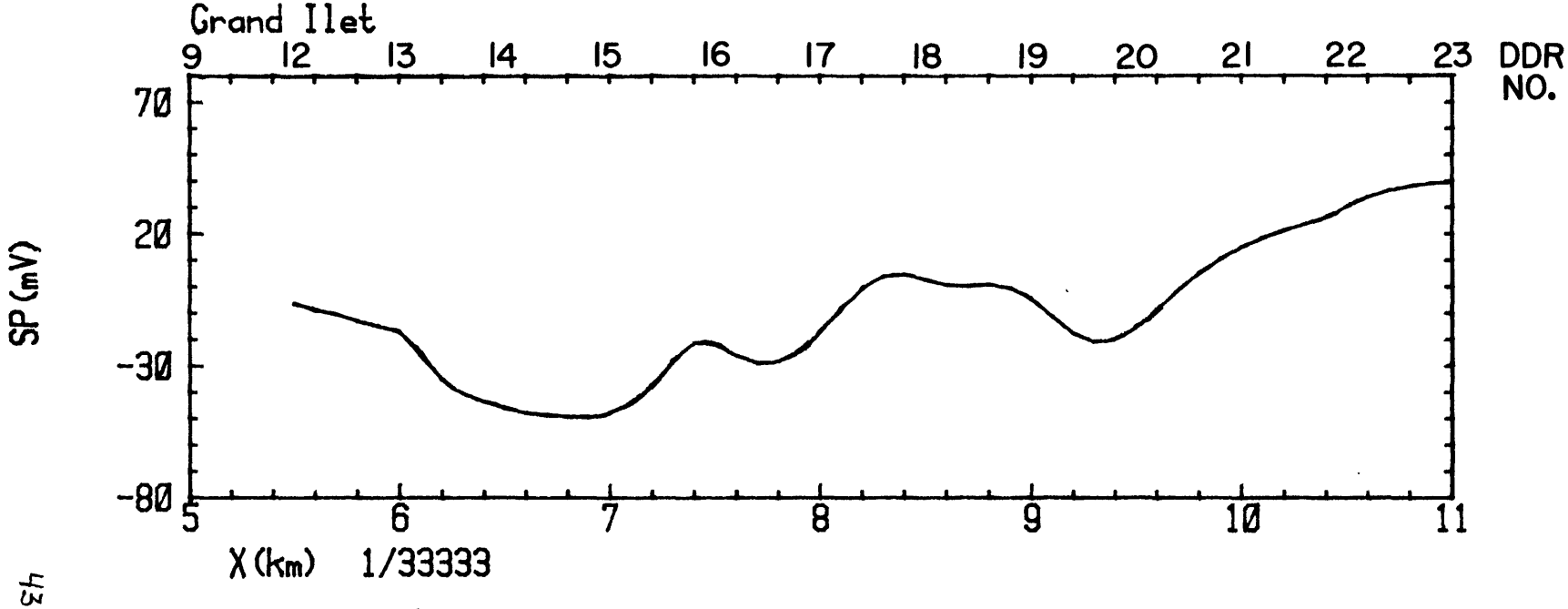

19. Projected SP and DDR data for Grand Ilet traverse. A topographic correlation of -0.163 mV/m has been removed from all but the last 2.35 km. An 8 point bi-directional running average filter has been used.

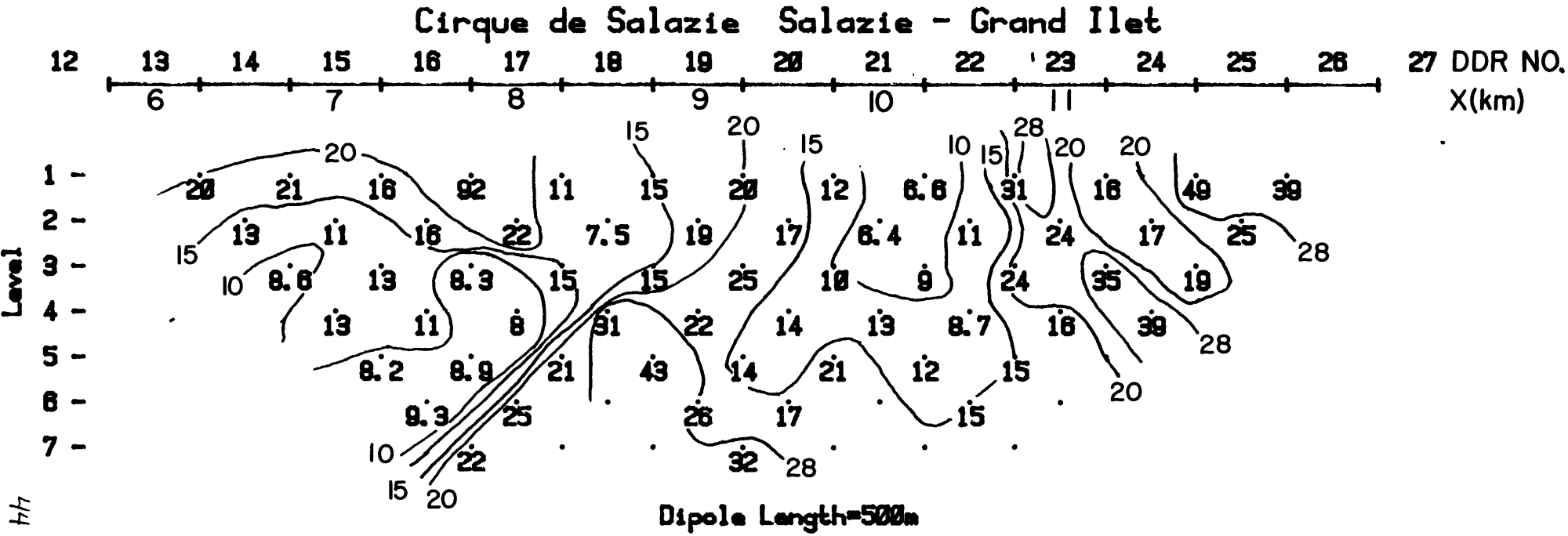
Cirque de Salazie Salazie - Grand Ilet
12 13 14 15 16 17 18 19 20 21 22 23 24 25 26 27 DDR NO.
6 7 8 9 10 11 X(km)
Level
1
2
3
4
5
6
7
Dipole Length=500m

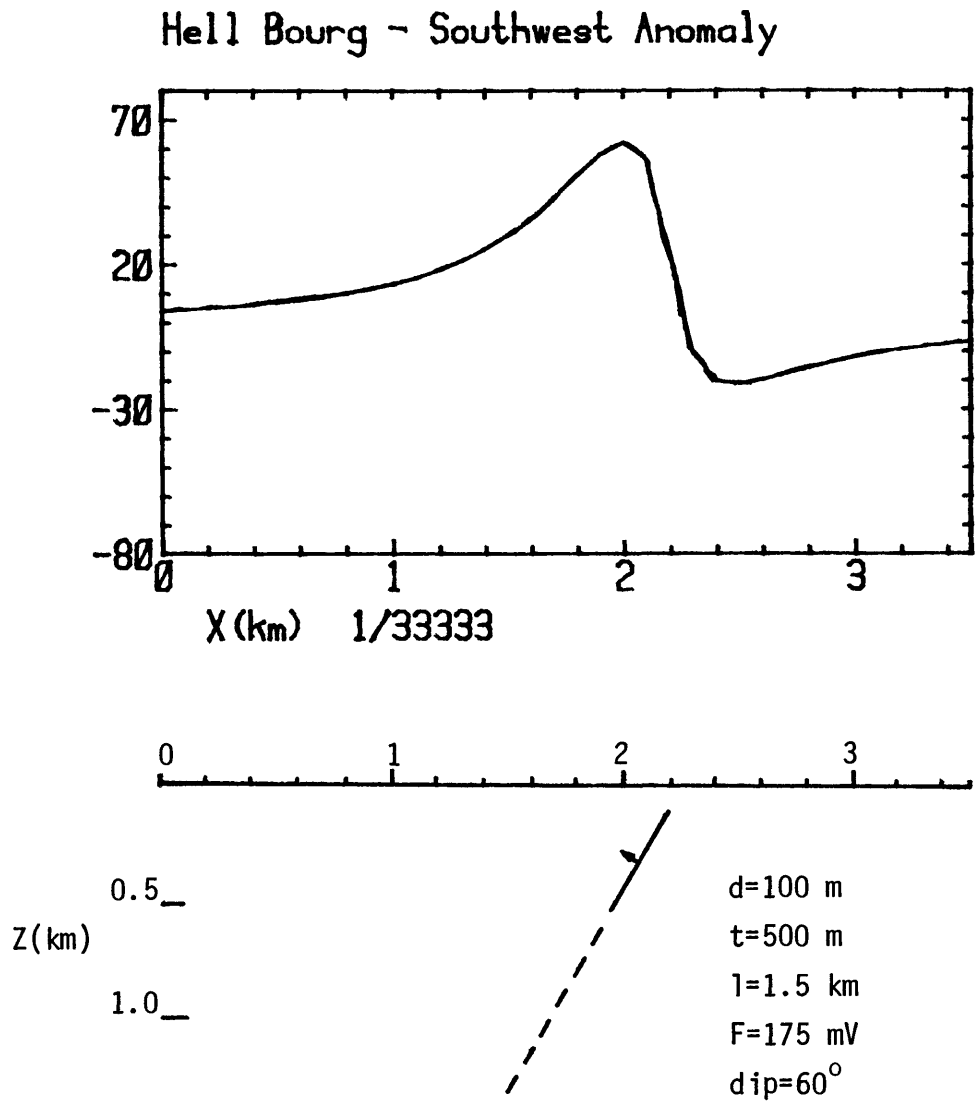

20. Model of southwest boundary anomaly on the Hell-Bourg profile.

The broad anomaly between 2.2 km and 6.5 km appears to be associated with the northeast boundary of the conductive zone with the zero crossing near an inferred material boundary. If the anomaly is caused by a thermoelectric source, it must be rather deep (~2 km) to produce the broad anomaly. This poses a dilemma as a source this deep could not produce the rapid drop in potential observed on either side of the peak (2.2 km) and of the trough (6.2 km).

The Grand Ilet DDR profile also shows a conductive zone on its east end which corresponds with the conductive region on the Hell-Bourg profile. However, the west boundary of this zone between stations 19 and 21 is not as well defined as the boundaries on the Hell-Bourg profile. A broad negative anomaly of moderate amplitude (-50 mV) is associated with the conductive region.

3.4 Summary of results

The following general comments can be made about the Salazie SP data:

1. A lower potential is associated with the conductive zones observed by the DDR data.
2. The anomalies tend to vary the most rapidly near the edges of the conductive zone.
3. The negative SP anomalies could be produced by a heat source associated with the conductive region if the thermoelectric properties of the conductive zone are less than those of the surrounding material.

Interpretation of the Salazie data without a better model of the conductivity structure will be difficult. A two dimensional interpretation of the DDR data would be helpful in this regard.

4. Conclusions

The two regions described in this report, Rivière Langevin and Cirque de Salazie, contrast each other in some important ways. Geologically the Rivière Langevin area is the younger being associated with Piton de la Fournaise, and is less eroded. The rocks are electrically resistive which in turn tends to produce large SP anomalies. This fact should not be confused with the extremely large voltages (>1000 mV) produced by the descent of water from the Plaine des Sables. Finally and most importantly, the electrical structure is relatively simple being composed primarily of layers which become more conductive with depth. In places where the conductive zone is shallower significant SP anomalies have been found.

By contrast the Cirque de Salazie is geologically older having been erosionally carved out of the Piton des Neiges volcanic system. The rocks are much more conductive, and as a result the measured SP anomalies are smaller. Topographic effects in the data are less extreme than at Rivière Langevin. As the electrical structure is complicated a two or three dimensional model is probably necessary to describe the data.

From a geothermal point of view, the Rivière Langevin data are the most interesting and the most interpretable. There are several large anomalies (300-1500 mV) which are most likely caused by the flow of subsurface water. These anomalies are associated with Piton Chisny, the south edge of the Plaine des Sables, and the Ravin de la Plaine des Sables. Farther south along the Rivière Langevin two SP anomalies have been identified which are not believed to be caused by a streaming potential mechanism. A model using a thermoelectric source mechanism has been developed which describes the anomalies, and corresponds with the resistivity data interpretation. The interpretation suggests that the geologic cause of the enhanced conductivity

is also the source region for the SP anomalies. Use of a thermoelectric source model would argue that these are zones of elevated temperature. The thermoelectric source is favored over a streaming potential source on the basis of a 200 m test well drilled near Grand Pays which was dry but hot. The absence of fluid which could be moved by convection argues against a streaming potential source.

The Cirque de Salazie data are less clear. The SP anomalies seem to be associated with resistivity boundaries as might be expected theoretically, but the correlation is not precise. Part of this problem is caused by the complex resistivity structure. Before a great deal more can be done with this data it will be necessary to make an interpretation of the DDR data.

Acknowledgment

This work was performed while I was a guest of the Département Géothermie of B.R.G.M. I would like to thank A. GERARD, L. STIELJES, P. PUVILLAND, J.-L. GELOT, Ph. LESAGE, and G. PETIAU for their assistance in making this work possible. Numerous discussions with V. BARTHES and J.-Ph. RANCON were of great help with regard to geophysical and geological interpretations.

References

Benderiter, Y., and Gérard, A., Etude audiomagnétotellurique de l'Ile de la Réunion en vue de l'évaluation de son potential géothermique, unpublished report, C.N.R.S., Garchy, 58150 Pouilly sur Loire and B.R.G.M., Départment Géothermie, B.P. 6009, 45018 Orléans, FRANCE, 1981.

Billard, Guy, Carte Géologique de la France, La Réunion, scale 1:50,000, B.R.G.M., Orléans, France, 1974.

Fitterman, D. V., Electrokinetic and magnetic anomalies associated with dilatant regions in a layered earth, J. Geophys. Res., 83, 5923-5928, 1978.

_____, Calculations of self-potential anomalies near vertical contacts, Geophysics, 44, 195-205, 1979.

Fitterman, D. V. and Corwin, R. F., Inversion of self-potential data from the Cerro Prieto geothermal field, Mexico, paper submitted to Geophysics, 1982.

Nourbehecht, B., Irreversible thermodynamic effects in inhomogeneous media and their application in certain geoelectric problems, Ph. D. thesis, MIT, Cambridge, 1963.

Petiau, G., and Dupis, A., Noise, temperature coefficient, and long term stability of electrodes for telluric observations, Geophys. Prosp., 28, 792-804, 1980.

Sill, W. R., Self potential modelling from primary sources, preprint, paper submitted to Geophysics, 1982.